Commun. Comput. Phys.
doi: 10.4208/cicp.OA-2016-0181

Vol. **22**, No. 2, pp. 542-571
August 2017

A Domain Decomposition Based Spectral Collocation Method for Lane-Emden Equations

Yuling Guo and Jianguo Huang*

School of Mathematical Sciences, and MOE-LSC, Shanghai Jiao Tong University, Shanghai 200240, P.R. China.

Received 25 October 2016; Accepted (in revised version) 15 January 2017

Abstract. A domain decomposition based spectral collocation method is proposed for numerically solving Lane-Emden equations, which are frequently encountered in mathematical physics and astrophysics. Compared with the existing methods, this method requires less computational cost and is particularly suitable for long-term computation. The related error estimates are also established, indicating the spectral accuracy of the method. The numerical performance and efficiency of the method are illustrated by several numerical experiments.

AMS subject classifications: 65L05, 65L06, 65L20

Key words: Multi-step Legendre-Gauss-Radau spectral collocation method, Volterra integro-differential equation, decomposition method, long-term computation, error estimates.

1 Introduction

The Lane-Emden equation is defined in the following form:

$$\begin{cases} u''(t)+\dfrac{a}{t}u'(t)+f(u(t))=0, \quad t>0, \ a\in\mathbb{N}^+, \\ u(0)=u_0, \quad u'(0)=0, \end{cases} \tag{1.1}$$

where u_0 is the initial data and f is a continuous function in $\mathbb{R}$. Such kind of equations are frequently encountered in mathematical physics and astrophysics, including the theory of stellar structure, the thermal behavior of a spherical cloud of gas, isothermal gas spheres, and the theory of thermionic currents. We refer the reader to the references [4, 11, 17] for details about the physical background of the equation.

*Corresponding author. *Email addresses:* jghuang@sjtu.edu.cn (J. Huang), guoyuling56@163.com (Y. Guo)

 ©2017 Global-Science Press

https://doi.org/10.4208/cicp.OA-2016-0181 Published online by Cambridge University Press

Due to the importance of Lane-Emden equations, there have developed a variety of numerical methods for solving them in the past decade (see [12,14,22] and the references therein). The typical and effective approach is the spectral method. Concretely speaking, Parand et al. proposed in [14] a Hermite function collocation method, Doha et al. proposed respectively in [5,6] a Jacobi rational Gauss collocation/pseudospectral method, and Gürbü and Sezer proposed in [7] a Laguerre collocation method, to solve the Lane-Emden type equations. The other recent methods include the homotopy perturbation method (cf. [13]), the variational iteration method (cf. [23]), the Adomian decomposition method (cf. [16]) and the wavelet method (cf. [18,26]).

Compared with the other methods, the spectral method has a significant advantage, that means, it can produce very accurate numerical solution (cf. [19]). However, all the spectral methods mentioned above only study the global approximation in the whole solution domain $[0,\infty)$. Hence, they are not suitable for long-term computation since we can not choose the polynomial degree N very large in actual computation (cf. [24]). The other point to be emphasized is that no error analysis has been developed for these methods. In this article, we aim to devise a domain decomposition based spectral collocation method for solving the problem (1.1), which is very suitable for long-term computation. Then, we will establish error estimates for the method and show it has spectral accuracy if the exact solution is smooth enough. Moreover, we will provide a series of numerical experiments to show the numerical performance of our method proposed.

Since the idea of the proposed domain decomposition spectral collocation method is very natural and intuitive, we'd like to briefly introduce it in this introduction section. The details of the method can be found in Section 3. To this end, we first divide the unbounded domain $[0,\infty)$ into the two subdomains $\Gamma_1:=[0,T_0]$ and $\Gamma_2:=[T_0,\infty)$, where T_0 is a given constant as desired. To tackle the singularity of the coefficient function a/t, we reformulate (1.1) as the initial value problem of an equivalent Volterra integro-differential equation:

$$\begin{cases} u'(t)+\displaystyle\int_0^t \frac{s^a}{t^a} f(u(s))ds=0, \quad t\in\Gamma_1, \\ u(0)=u_0, \end{cases} \tag{1.2}$$

together with the initial value problem of a second order differential equation

$$\begin{cases} u''(t)+\dfrac{a}{t}u'(t)+f(u(t))=0, \quad t\in\Gamma_2, \\ u(T_0)=u_(T_0-), \quad u'(T_0)=u'(T_0-), \end{cases} \tag{1.3}$$

where $u(T_0-)$ and $u'(T_0-)$ are determined from problem (1.2). Then, the problem (1.2) is approximated by a multi-step Legendre-Gauss-Radau (LGR) collocation method based on the formulation (1.2) (cf. [2,20]). Since the previous method is very time-consuming, we then turn to use the standard multi-step LGR collocation method for solving the problem (1.1) after $t\geq T_0$, i.e. the problem (1.3) (cf. [10]). We remark that, compared with the

https://doi.org/10.4208/cicp.OA-2016-0181 Published online by Cambridge University Press

spectral collocation method in [10], we use here the Legendre-Gauss-Radau collocation points instead of the Legendre-Gauss collocation points, so that we can determine the initial values of a problem to be solved in a subinterval from the computed results directly. This will increase the efficiency of the implementation. We mention in passing that the domain decomposition methods are a very effective tool to solve a variety of differential equations whose coefficient functions are singular or degenerate around the boundary of the solution domain, since we can use different suitable and efficient spectral methods in different domains. We refer to [8] for details along this line.

In order to derive the error estimates of the proposed spectral collocation method, we require first to establish error estimates for the multi-step LGR collocation method based on the formulation (1.2) and the LGR collocation method for the method (1.3). The estimates can be developed by using some ideas in [10, 21] combined with technical derivation handling the choice of Legendre-Gauss-Radau collocation points. The combination of all these estimates will lead to the error analysis of our method developed here readily. The details can be found in the appendix of this article.

The rest of this article is organized as follows. In Section 2, we introduce some basic properties of the shifted Legendre polynomial interpolations. In Section 3, we develop a domain decomposition based spectral collocation method for solving the Lane-Emden equation (1.1). In Section 4, we mention the error estimates for the proposed collocation methods, with the detailed proofs given as an appendix. In Section 5, we report our numerical findings and demonstrate the accuracy of the proposed method by considering several numerical examples. Some concluding statements are given in Section 6.

2 The properties of the shifted Legendre polynomial interpolations

In this section, we introduce some basic properties of the shifted Legendre polynomial interpolations for later uses. Let I_h be a partition of $[0,\infty)$ given by

$$I_h := \{t_n:\ 0=t_0<t_1<\cdots<t_{N_0}=T_0<\cdots<t_N=T<t_{N+1}<\cdots\}; \tag{2.1}$$

write $I_n := (t_{n-1},t_n]$ and $h_n := t_n - t_{n-1}$. Let $L_l(x)$, $x\in[-1,1]$ be the standard Legendre polynomial of degree l (cf. [19]). Then, the shifted Legendre polynomial $L_{n,l}(t)$, $t\in I_n$ is defined by

$$L_{n,k}(t) = L_k\Big(\frac{2t-t_{n-1}-t_n}{h_n}\Big), \quad t\in I_n, \quad k\geq 0.$$

The set of $L_{n,k}(t)$, $k\geq 0$ is a complete $L^2(I_n)$-orthogonal system, i.e.,

$$\int_{I_n} L_{n,k}(t)L_{n,j}(t)dt = \frac{h_n}{2k+1}\delta_{k,j}, \tag{2.2}$$

https://doi.org/10.4208/cicp.OA-2016-0181 Published online by Cambridge University Press

where $\delta_{k,j}$ is the usual Kronecker delta. Thus for any $v\in L^2(I_n)$, we can write

$$v(t)=\sum_{k=0}^{\infty}v_{n,k}L_{n,k}(t),\quad v_{n,k}=\frac{2k+1}{h_n}\int_{I_n}v(t)L_{n,k}(t)dt. \tag{2.3}$$

According to the properties of the standard Legendre polynomials, we have (cf. [19]) that for $k\geq 1$ there hold

$$\begin{aligned}&(k+1)L_{n,k+1}(t)-h_n^{-1}(2k+1)(2t-t_{n-1}-t_n)L_{n,k}(t)+kL_{n,k-1}(t)=0,\\&L'_{n,k+1}(t)-L'_{n,k-1}(t)=\frac{4k+2}{h_n}L_{n,k}(t).\end{aligned} \tag{2.4}$$

In particular,

$$\begin{aligned}&L_{n,0}(t)=1,\qquad L_{n,1}(t)=\frac{2t-t_{n-1}-t_n}{h_n},\\&L_{n,2}(t)=\frac{6t^2-6(t_{n-1}+t_n)t+4t_{n-1}t_n+t_{n-1}^2+t_n^2}{h_n^2}.\end{aligned} \tag{2.5}$$

Furthermore, we can deduce from (2.4) that for $k\geq 2$,

$$\frac{4}{h_n^2}L_{n,k}(t)=\frac{L''_{n,k+2}(t)}{(2k+3)(2k+1)}-\frac{2L''_{n,k}(t)}{(2k+3)(2k-1)}+\frac{L''_{n,k-2}(t)}{(2k+1)(2k-1)}. \tag{2.6}$$

We now turn to the right-hand Legendre-Gauss-Radau interpolation. Let $\{x_{n,j},\omega_{n,j}\}_{j=0}^{M_n}$ be the nodes (arranged in ascending order with the fixed right endpoint $x_{n,M_n}=1$) and the corresponding Christoffel numbers of the standard Legendre-Gauss-Radau interpolation on the interval $[-1,1]$.

Let $\mathcal{P}_{M_n}(I_n)$ be the set of polynomials of degree no more than M_n on the interval I_n. Introduce

$$t_{n,j}:=\frac{1}{2}(h_nx_{n,j}+t_{n-1}+t_n),\qquad 0\leq j\leq M_n.$$

Then, thanks to the property of the standard Legendre-Gauss-Radau quadrature, it follows that

$$\int_{I_n}\phi(t)dt=\frac{h_n}{2}\int_{-1}^{1}\phi\Big(\frac{h_nx+t_{n-1}+t_n}{2}\Big)dx=\frac{h_n}{2}\sum_{j=0}^{M_n}\phi(t_{n,j})\omega_{n,j},\quad\forall\phi(t)\in\mathcal{P}_{2M_n}(I_n). \tag{2.7}$$

Next we define the discrete inner product and norm over I_n as follows

$$\langle u,v\rangle_{I_n}:=\frac{h_n}{2}\sum_{j=0}^{M_n}u(t_{n,j})v(t_{n,j})\omega_{n,j},\quad \|u\|_{I_n,M_n}:=\langle u,u\rangle_{I_n}^{\frac{1}{2}}. \tag{2.8}$$

https://doi.org/10.4208/cicp.OA-2016-0181 Published online by Cambridge University Press

We denote by $\mathcal{I}_{t,M_n}v\in\mathcal{P}_{M_n}(I_n)$ the shifted Legendre-Gauss-Radau interpolation operator. That means for $v\in C(\overline{I_n})$,

$$\mathcal{I}_{t,M_n}v(t_{n,j})=v(t_{n,j}),\quad 0\le j\le M_n.$$

Then it is evident from (2.7) and (2.8) that

$$\int_{I_n}\mathcal{I}_{t,M_n}(u(t)v(t))dt=\frac{h_n}{2}\sum_{j=0}^{M_n}u(t_{n,j})v(t_{n,j})\omega_{n,j}=\langle u,v\rangle_{I_n}.$$

3 A domain decomposition based spectral collocation method

In this section, we intend to introduce a domain decomposition based spectral collocation method for solving the Lane-Emden equation (1.1). Essentially, it is a combination of two LGR spectral collocation schemes for second order differential equations. The first method is a collocation method (cf. [2]) based on its Volterra integro-differential equation (VIDE) (cf. (1.2)). Observing that this method is very time-consuming, we next propose a domain decomposition based LGR spectral collocation method. The idea of the method is very simple and natural. Since the coefficient function a/t in Eq. (1.1) has singularity at $t=0$, we still use the previous method for discretization around $t=0$. After the time T_0, which is a given number as desired, we turn to use the standard multi-step LGR spectral collocation method for solving the second order differential equation (1.1). In this time interval, the coefficient function becomes smooth, so this method is able to approximate the exact solution very well. After careful and detailed reasoning, it is shown that the errors of both methods have spectral accuracy. However, the latter method require much less computational cost than the foregoing one.

3.1 A LGR collocation scheme based on the VIDE

Denote by $u_n(t)$ the solution of (1.1) on the n-th element, i.e.,

$$u_n(t):=u(t)|_{I_n},\quad n\ge 1.$$

First of all, as shown in Section 1, the integral equation (1.2) can be recast as follows.

For any $t\in I_n$,

$$\frac{d}{dt}u_n(t)+\sum_{k=1}^{n-1}\int_{I_k}\frac{s^a}{t^a}f(u_k(s))ds+\frac{t-t_{n-1}}{h_n}\int_{I_n}\frac{[\sigma(\lambda,t)]^a}{t^a}f(u_n(\sigma(\lambda,t)))d\lambda=0,\qquad(3.1)$$

where

$$\xi=\sigma(\lambda,t):=t_{n-1}+\frac{(\lambda-t_{n-1})(t-t_{n-1})}{h_n},\qquad\lambda\in I_n.$$

https://doi.org/10.4208/cicp.OA-2016-0181 Published online by Cambridge University Press

Based on this formulation, the LGR collocation scheme for solving (1.1) is to seek $U_n(t)\in\mathcal{P}_{M_n+1}(I_n)$, such that

$$\begin{cases}\dfrac{d}{dt}U_n(t)+\displaystyle\sum_{k=1}^{n-1}\left\langle\frac{s^a}{t^a},f(U_k)\right\rangle_{I_k}+\frac{t-t_{n-1}}{h_n}\left\langle\frac{[\sigma(\cdot,t)]^a}{t^a},f(U_n(\sigma(\cdot,t)))\right\rangle_{I_n}=0,\ \ t\in\{t_{n,j}\}_{j=0}^{M_n},\\ U_n(t_{n-1})=U_{n-1}(t_{n-1}),\end{cases}\tag{3.2}$$

where $U_k(t)\in\mathcal{P}_{M_k+1}(I_k)$ is the numerical solution of $u_k(t)$ on the interval I_k, and $U_1(t_0)=u_0$. In the following, we express the collocation method in continuous version by using the interpolation operator $\mathcal{I}_{t,M_n}$, instead of the pointwise form (cf. [2]), which is more convenient for us to develop the solution algorithm and theoretical analysis.

$$\begin{cases}\dfrac{d}{dt}U_n(t)+\mathcal{I}_{t,M_n}\left[\displaystyle\sum_{k=1}^{n-1}\left\langle\frac{s^a}{t^a},f(U_k)\right\rangle_{I_k}+\frac{t-t_{n-1}}{h_n}\left\langle\frac{[\sigma(\cdot,t)]^a}{t^a},f(U_n(\sigma(\cdot,t)))\right\rangle_{I_n}\right]=0,\\ U_n(t_{n-1})=U_{n-1}(t_{n-1}).\end{cases}\tag{3.3}$$

Next, let us discuss how to solve the scheme (3.3) effectively at each time interval I_n. As usual, to ensure stability of the solution, we carry out the computation in the frequency space. In other words, we express the unknown function $U_n(t)$ in the form

$$U_n(t)=\sum_{p=0}^{M_n+1}\widehat{u}_p^nL_{n,p}(t),\tag{3.4}$$

which implies

$$\frac{d}{dt}U_n(t)=\sum_{p=1}^{M_n+1}\widehat{u}_p^nL'_{n,p}(t).\tag{3.5}$$

Set

$$\mathcal{I}_{t,M_n}\mathcal{I}_{s,M_k}\left[\frac{s^a}{t^a}f(U_k(s))\right]=\sum_{p=0}^{M_n}\sum_{p'=0}^{M_k}a_{p,p'}^kL_{n,p}(t)L_{k,p'}(s),\tag{3.6}$$

$$\mathcal{I}_{t,M_n}\mathcal{I}_{\lambda,M_n}\left[(t-t_{n-1})\frac{[\sigma(\lambda,t)]^a}{t^a}f(U_n(\sigma(\lambda,t)))\right]=\sum_{p,p'=0}^{M_n}b_{p,p'}^nL_{n,p}(t)L_{n,p'}(\lambda).\tag{3.7}$$

Then it follows from (2.2) and (3.6) that, for $1\le k\le n-1$,

$$\int_{I_k}\mathcal{I}_{t,M_n}\mathcal{I}_{s,M_k}\left[\frac{s^a}{t^a}f(U_k(t))\right]ds=\sum_{p=0}^{M_n}\sum_{p'=0}^{M_k}a_{p,p'}^kL_{n,p}(t)\int_{I_k}L_{k,p'}(s)\cdot1ds=h_k\sum_{p=0}^{M_n}a_{p,0}^kL_{n,p}(t).\tag{3.8}$$

https://doi.org/10.4208/cicp.OA-2016-0181 Published online by Cambridge University Press

That means, $\{h_k a^k_{p,0}\}_p$ are the coefficients of the function on the left of (3.8) expanded by the Legendre polynomials $\{L_{n,p}(t)\}_p$. Hence, we have by (2.3) and (2.7) that

$$a^k_{p,0}=\frac{2p+1}{4}\sum_{i=0}^{M_n}\sum_{j=0}^{M_k}\frac{t^a_{k,j}}{t^a_{n,i}}f(U_k(t_{k,j}))L_{n,p}(t_{n,i})\omega_{k,j}\omega_{n,i},\quad 0\le p\le M_n. \tag{3.9}$$

On the other hand, owing to (2.4) and using some direct manipulation, we find Eq. (3.8) can be rewritten as

$$\int_{I_k}\mathcal{I}_{t,M_n}\mathcal{I}_{s,M_k}\Big[\frac{s^a}{t^a}f(U_k(t))\Big]ds=h_k\sum_{p=0}^{M_n}a^k_{p,0}L_{n,p}(t)=h_kh_n\sum_{p=1}^{M_n+1}\widehat{a}^k_{p,0}L'_{n,p}(t), \tag{3.10}$$

where

$$\begin{aligned}&\widehat{a}^k_{p,0}=\frac{a^k_{p-1,0}}{4p-2}-\frac{a^k_{p+1,0}}{4p+6},\quad 1\le p\le M_n-1,\\ &\widehat{a}^k_{M_n,0}=\frac{a^k_{M_n-1,0}}{4M_n-2},\quad \widehat{a}^k_{M_n+1,0}=\frac{a^k_{M_n,0}}{4M_n+2}.\end{aligned} \tag{3.11}$$

Employing the similar argument as above, we can also obtain

$$\begin{aligned}&\int_{I_n}\mathcal{I}_{t,M_n}\mathcal{I}_{\lambda,M_n}\Big[(t-t_{n-1})\frac{[\sigma(\lambda,t)]^a}{t^a}f(U_n(\sigma(\lambda,t)))\Big]d\lambda\\ =&h_n\sum_{p=0}^{M_n}b^n_{p,0}L_{n,p}(t)=h_n^2\sum_{p=1}^{M_n+1}\widehat{b}^n_{p,0}L'_{n,p}(t),\end{aligned} \tag{3.12}$$

where

$$\begin{aligned}&b^n_{p,0}=\frac{2p+1}{4}\sum_{i,j=0}^{M_n}(t_{n,i}-t_{n-1})\frac{\sigma^a_{i,j}}{t^a_{n,i}}f(U_n(\sigma_{i,j}))L_{n,p}(t_{n,i})\omega_{n,j}\omega_{n,i},\quad 0\le p\le M_n,\\ &\sigma_{i,j}=\sigma(t_{n,j},t_{n,i}),\\ &\widehat{b}^n_{p,0}=\frac{b^n_{p-1,0}}{4p-2}-\frac{b^n_{p+1,0}}{4p+6},\quad 1\le p\le M_n-1,\\ &\widehat{b}^n_{M_n,0}=\frac{b^n_{M_n-1,0}}{4M_n-2},\quad \widehat{b}^n_{M_n+1,0}=\frac{b^n_{M_n,0}}{4M_n+2}.\end{aligned} \tag{3.13}$$

Now, inserting (3.5), (3.10) and (3.12) into (3.3), we arrive at

$$\sum_{p=1}^{M_n+1}\widehat{u}^n_pL'_{n,p}(t)+h_n\sum_{k=1}^{n-1}h_k\sum_{p=1}^{M_n+1}\widehat{a}^k_{p,0}L'_{n,p}(t)+h_n\sum_{p=1}^{M_n+1}\widehat{b}^n_{p,0}L'_{n,p}(t)=0. \tag{3.14}$$

https://doi.org/10.4208/cicp.OA-2016-0181 Published online by Cambridge University Press

Observing that $\{L'_{n,p}\}_p$ are orthogonal polynomials with respect to the weight function $1-t^2$, we know the coefficients of $L'_{n,p}$ of the function on the left of (3.14) must vanish. We therefore have

$$\widehat{u}_p^n = -h_n \sum_{k=1}^{n-1} h_k \widehat{a}_{p,0}^k - h_n \widehat{b}_{p,0}^n, \qquad 1 \le p \le M_n + 1. \tag{3.15}$$

Furthermore, due to $L_{n,p}(t_{n-1}) = (-1)^p$ and using the initial condition of the problem (3.3), we can get from (3.4) that

$$\widehat{u}_0^1 = u_0 - \sum_{p=1}^{M_n+1} (-1)^p \widehat{u}_p^1, \qquad \widehat{u}_0^n = U_{n-1}(t_{n-1}) - \sum_{p=1}^{M_n+1} (-1)^p \widehat{u}_p^n, \quad n \ge 2. \tag{3.16}$$

According to the relations (3.4), (3.9), (3.11), (3.13), (3.15) and (3.16), we can derive a fixed point formulation for the coefficients $\{\widehat{u}_p^n\}_p$, which naturally leads to the following fixed point algorithm for solving the previous coefficients, described as Algorithm 1.

Algorithm 1 The fixed point iterative algorithm

for $n = 1, \cdots, N$ **do**
  Input: set the initial guess of $\{\widehat{u}_p^n\}_{p=0}^{M_n+1}$ to be any given numbers, say zero values;
  if $n > 1$ **then**
    for $k = 1, \cdots, n-1$, **do**
      Compute $\widehat{a}_{p,0}^k$ by (3.9) and (3.11);
    end for
  end if
  while the maximum absolute difference between two consecutive coefficients of $\{\widehat{u}_p^n\}_{p=0}^{M_n+1}$ is bigger than the desired tolerance **do**
    Compute $\{U_n(t_{n,i})\}_{i=0}^{M_n}$ and $\{U_n(\sigma(t_{n,j}, t_{n,i}))\}_{0 \le i \le M_n,\ 0 \le j \le M_n}$ by (3.4);
    Compute $\{\widehat{b}_{p,0}^n\}_{p=0}^{M_n}$ by (3.13);
    Update the coefficients $\{\widehat{u}_p^n\}_{p=0}^{M_n+1}$ by (3.15) and (3.16);
  end while
  Compute the values $\{U_n(t_{n,j})\}_{j=0}^{M_n}$ by (3.4);
end for

3.2 A domain decomposition based LGR spectral collocation method

The advantage of Algorithm 1 is that it can solve the problem (1.1) with high accuracy, even if the coefficient function a/t is singular at $t = 0$. The disadvantage is that when solving the numerical solution on the subinterval I_n, we require to compute repeatedly the numerical integration over the previous $n-1$ subintervals $I_1, I_2, \cdots, I_{n-1}$. So the algorithm is very time-consuming and is in particular not suitable for long-term computation.

https://doi.org/10.4208/cicp.OA-2016-0181 Published online by Cambridge University Press

Our numerical experiment in Section 5 will also show this weakness. Based on this observation, we aim to design a domain decomposition based spectral method to overcome this difficulty. To this end, we choose $T_0 = t_N$ as desired, and then solve the problem (1.1) after $t \geq T_0$ by means of the direct spectral method for solving second order differential equations as given in [10]. The only difference is that we use the Legendre-Gauss-Radau collocation points instead of the Legendre-Gauss collocation points, in order to increase the efficiency of the implementation. Mathematically speaking, we want to seek $U_n(t) \in \mathcal{P}_{M_n+2}(I_n)$ $(n \geq N+1)$ such that

$$\begin{cases} U_n''(t)+\dfrac{a}{t}U_n'(t)+f(U_n(t))=0, \quad t\in\{t_{n,j}\}_{j=0}^{M_n}, \\ U_n(t_{n-1})=U_{n-1}(t_{n-1}), \quad U_n'(t_{n-1})=U_{n-1}'(t_{n-1}). \end{cases} \tag{3.17}$$

It should be emphasized that the initial values of $U_N(t_N)$ and $U_N'(t_N)$ are obtained from Algorithm 1. Next, let us describe the above method in continuous setting for further discussion. As a matter of fact, with the help of the interpolation operator $\mathcal{I}_{t,M_n}$, we can reformulate the first equation of (3.17) as

$$U_n''(t)=\mathcal{I}_{t,M_n}F_n(t,U_n(t),U_n'(t)), \quad t\in I_n, \tag{3.18}$$

where

$$F_n(t,U_n(t),U_n'(t))=-\frac{a}{t}U_n'(t)-f(U_n(t)).$$

Then we need to design an effective algorithm for solving (3.18) at each time interval I_n. To this end, we express the unknown function $U_n(t)$ in the form

$$U_n(t)=\sum_{p=0}^{M_n+2}\widetilde{u}_p^n L_{n,p}(t), \tag{3.19}$$

which implies

$$U_n'(t)=\sum_{p=1}^{M_n+2}\widetilde{u}_p^n\partial_t L_{n,p}(t), \quad U_n''(t)=\sum_{p=2}^{M_n+2}\widetilde{u}_p^n\partial_t^2 L_{n,p}(t). \tag{3.20}$$

Set

$$\mathcal{I}_{t,M_n}F_n(t,U_n(t),U_n'(t))=\sum_{p=0}^{M_n}\widetilde{f}_p^n L_{n,p}(t). \tag{3.21}$$

The combination of (3.21) with (2.3) and (2.7) implies

$$\widetilde{f}_p^n=\frac{2p+1}{2}\sum_{j=0}^{M_n}F_n(t_{n,j},U_n(t_{n,j}),U_n'(t_{n,j}))L_{n,p}(t_{n,j})\omega_{n,j}, \quad 0\leq p\leq M_n. \tag{3.22}$$

https://doi.org/10.4208/cicp.OA-2016-0181 Published online by Cambridge University Press

On the other hand, by (2.5), (2.6) and some direct manipulation, we find the relation (3.21) can be rewritten as

$$\mathcal{I}_{t,M_n}F_n(t,U_n(t),U_n'(t))=\sum_{p=0}^{M_n}\widetilde{f}_p^n L_{n,p}(t)=\sum_{p=2}^{M_n+2}\widehat{f}_p^n\partial_t^2 L_{n,p}(t), \tag{3.23}$$

where

$$\begin{aligned}
&\widehat{f}_p^n=\frac{h_n^2}{4}\Big[\frac{\widetilde{f}_{p-2}^n}{(2p-3)(2p-1)}-\frac{2\widetilde{f}_p^n}{(2p-1)(2p+3)}+\frac{\widetilde{f}_{p+2}^n}{(2p+3)(2p+5)}\Big],\quad 2\le p\le M_n-2,\\
&\widehat{f}_{M_n-1}^n=\frac{h_n^2}{4}\Big[\frac{\widetilde{f}_{M_n-3}^n}{(2M_n-5)(2M_n-3)}-\frac{2\widetilde{f}_{M_n-1}^n}{(2M_n-3)(2M_n+1)}\Big],\\
&\widehat{f}_{M_n}^n=\frac{h_n^2}{4}\Big[\frac{\widetilde{f}_{M_n-2}^n}{(2M_n-3)(2M_n-1)}-\frac{2\widetilde{f}_{M_n}^n}{(2M_n-1)(2M_n+3)}\Big],\\
&\widehat{f}_{M_n+1}^n=\frac{h_n^2}{4}\frac{\widetilde{f}_{M_n-1}^n}{(2M_n-1)(2M_n+1)},\\
&\widehat{f}_{M_n+2}^n=\frac{h_n^2}{4}\frac{\widetilde{f}_{M_n}^n}{(2M_n+1)(2M_n+3)}.
\end{aligned} \tag{3.24}$$

Inserting (3.20) and (3.23) into (3.18) yields

$$\sum_{p=2}^{M_n+2}\widetilde{u}_p^n\partial_t^2 L_{n,p}(t)=\sum_{p=2}^{M_n+2}\widehat{f}_p^n\partial_t^2 L_{n,p}(t). \tag{3.25}$$

Due to the orthogonality of $\{\partial_t^2 L_{n,p}(t)\}_{P=2}^{M_n+2}$, and comparing the coefficients of $\partial_t^2 L_{n,p}(t)$ on both sides of (3.25), we know

$$\widetilde{u}_p^n=\widehat{f}_p^n,\quad 2\le p\le M_n+2. \tag{3.26}$$

Furthermore, the fact (cf. (3.177a) of [19])

$$L_{n,p}(0)=(-1)^p,\quad \partial_t L_{n,p}(0)=\frac{1}{h_n}(-1)^{p-1}p(p+1),\quad p\ge 0,$$

along with the initial condition in (3.17) gives

$$\begin{aligned}
\widetilde{u}_1^n&=\frac{h_n}{2}U_{n-1}'(t_{n-1})-\frac{1}{2}\sum_{p=2}^{M_n+2}(-1)^{p-1}p(p+1)\widetilde{u}_p^n,\\
\widetilde{u}_0^n&=U_{n-1}(t_{n-1})-\sum_{p=1}^{M_n+2}(-1)^p\widetilde{u}_p^n.
\end{aligned} \tag{3.27}$$

According to the relations (3.19), (3.20), (3.22), (3.24), (3.26) and (3.27), we can derive a fixed point formulation for the coefficients $\{\widetilde{u}_p^n\}_p$, which naturally leads to the following fixed point algorithm for solving the previous coefficients, described as Algorithm 2.

https://doi.org/10.4208/cicp.OA-2016-0181 Published online by Cambridge University Press

Algorithm 2 The fixed point iterative algorithm

Load the initial values $U_N(T_0)$ and $U'_N(T_0)$ computed by Algorithm 1;
for $n=N+1,\cdots,N_m$ **do**
  Input: set the initial guess of $\{\widetilde{u}_p^n\}_{p=0}^{M_n+2}$ to be any given numbers, say zero values;
  while the maximum absolute difference between two consecutive coefficients of $\{\widetilde{u}_p^n\}_{p=0}^{M_n+2}$ is bigger than the desired tolerance **do**
    Compute $\{U_n(t_{n,j})\}_{i=0}^{M_n}$ and $\{U'_n(t_{n,j})\}_{0\le i\le M_n}$ by (3.19) and (3.20);
    Compute $\{\widehat{f}_p^n\}_{p=2}^{M_n+2}$ by (3.22) and (3.24);
    Update the coefficients $\{\widetilde{u}_p^n\}_{p=0}^{M_n+2}$ by (3.26) and (3.27);
  end while
  Compute the values $\{U_n(t_{n,j})\}_{j=0}^{M_n}$ by (3.19);
end for

4 Error estimates for the proposed spectral collocation schemes

In this section, we only give the error estimates for the LGR collocation schemes (3.3) and (3.17), respectively. Since the proofs are rather lengthy, we leave them in the appendix to make the presentation more clear. Write $M:=\min_{n\ge1}M_n$ and $h:=\max_{n\ge1}h_n$. Assume that $u|_{I_n}\in H^r(I_n)$ and $f\in H^r(I_n)$ for $n\ge1$, and the function f used in (1.1) fulfills the following uniformly Lipschitz condition: there exists a positive constant L such that

$$|f(x_1)-f(x_2)|\le L|x_1-x_2|,\quad \forall x\in\mathbb{R}. \tag{4.1}$$

Theorem 4.1 (Error estimates for Algorithm 1)**.** *Let u be the solution of* (1.1) *and U be the numerical solution obtained by Algorithm 1, respectively. Given any $T>0$, assume that the mesh sizes h_n of the partition I_h in* (2.1) *satisfy* (A.18) *for $1\le n\le N$. Then there hold*

$$\|u-U\|^2_{H^1(0,T)}\le E_T,\quad |u(T)-U(T)|^2\le E_T,\quad |u'(T)-U'(T)|^2\le E'_T,$$

with

$$E_T:=\exp(cT^2L^2)\big[TM^{2-2r}h^{2r-2}\|\partial_t^r u\|^2_{L^2(0,T)}+T^2M^{-2r}h^{2r-2a}\|f(u(\cdot))\|^2_{H^r(0,T)}\big], \tag{4.2}$$

$$E'_T:=\exp(cT^2L^2)\big[T^2M^{2-2r}h^{2r-2}\|\partial_t^r u\|^2_{L^2(0,T)}+T^3M^{-2r}h^{2r-2a}\|f(u(\cdot))\|^2_{H^r(0,T)}\big], \tag{4.3}$$

where r is an integer such that $2\le r\le M_n+1$ and c is a generic constant.

Theorem 4.2 (Error estimates for Algorithm 2)**.** *Let u be the solution of* (1.1) *and U be the numerical solution obtained by Algorithm 2, respectively. Given any T, $T_0>0$ with $T>T_0$, assume that the mesh sizes h_n of the partition I_h in* (2.1) *satisfy* (A.18) *for $1\le n\le N_0$ and* (A.40)

https://doi.org/10.4208/cicp.OA-2016-0181 Published online by Cambridge University Press

for $N_0+1\leq n\leq N$, respectively. Then there hold

$$\begin{aligned}
&\|(u-U)\|^2_{H^2[0,T]}\leq cTh^{2r-3}M^{7-2r}\|\partial_t^r u\|^2_{L^2[T_0,T]}+cTE'_{T_0}+cTE_{T_0},\\
&|u(T)-U(T)|^2\leq ch^{2r-1}M^{7-2r}\|\partial_t^r u\|^2_{L^2[T_0,T]}+cE_{T_0}+ch^2E'_{T_0},\\
&|u'(T)-U'(T)|^2\leq ch^{2r-3}M^{7-2r}\|\partial_t^r u\|^2_{L^2[T_0,T]}+cE'_{T_0}+ch^2E_{T_0},
\end{aligned}$$

where r is an integer such that $3\leq r\leq M_n+1$, c is a generic constant, E_{T_0} and E'_{T_0} are determined by (4.2) *only with T replaced by T_0.*

From the above theorems we can conclude that both spectral collocation methods proposed in Section 3 (i.e. Algorithm 1 and Algorithm 2) exhibit the spectral accuracy if the exact solution u is sufficiently smooth. Our numerical results given in the next section also demonstrate such results.

5 Numerical results

In this section, we perform several numerical results to illustrate the efficiency of the proposed methods. We comment that when using Algorithm 1 or 2 to do numerical simulation, we always choose the initial guess to be zero values.

Example 5.1. Consider the following nonlinear Lane-Emden-type equation

$$\begin{cases} u''(t)+\dfrac{2}{t}u'+4(2e^u+e^{\frac{u}{2}})=0, \quad t>0,\\ u(0)=0, \quad u'(0)=0, \end{cases} \tag{5.1}$$

which has the exact solution:

$$u=-2\ln(1+x^2).$$

Let

$$E_{max[0,T]}:=\max_{0\leq t\leq T}|u(t)-U(t)|\approx\max_{1\leq n\leq N}|u(t_n)-U(t_n)|.$$

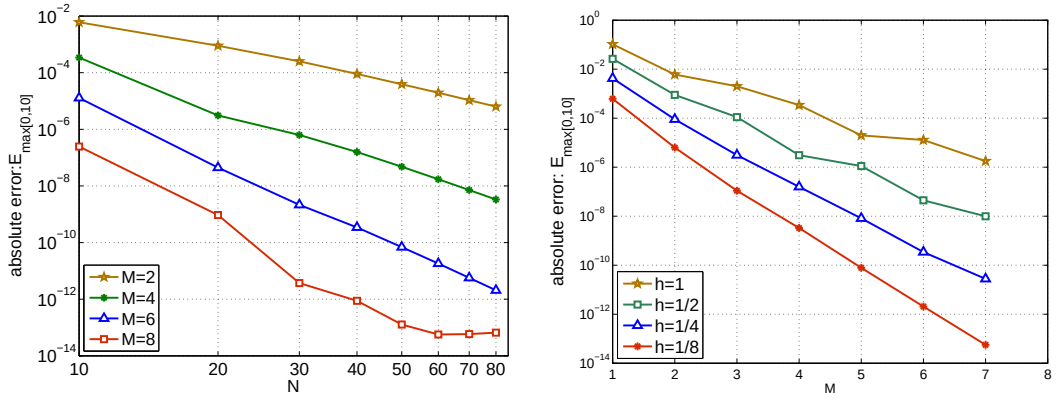
We use Algorithm 1 to solve (5.1) with $t\in[0,10]$, $N=1$ and $M=30$. That means a single-step collocation method with 31 collocation points is used for simulation. In Table 1, we list the errors of LGR collocation method (i.e. Algorithm 1), HFC method (cf. [14]) and SJC method (cf. [1]) at the corresponding points. The displayed results show that the LGR spectral collocation method has much higher computational accuracy than the other two methods.

Moreover, we use Algorithm 1 to solve Example 5.1 with various step sizes h and fixed $M=2,4,6,8$. The corresponding results are shown in Fig. 1(a), which indicate that the errors decay algebraically with refined time partitions. In Fig. 1(b), we plot the errors $E_{max[0,10]}$ with the variation of M and the fixed time step sizes $h=1,1/2,1/4,1/8$, from which we may observe that the numerical errors decay exponentially as M increases.

https://doi.org/10.4208/cicp.OA-2016-0181 Published online by Cambridge University Press

Table 1: Absolute errors of LGR method, HFC method and SJC method for Example 1 with 31 collocation points.

t	HFC-error	SJC-error	LGR-error
0.01	$2.93\cdot10^{-6}$	$6.31\cdot10^{-9}$	$2.33\cdot10^{-17}$
0.1	$3.94\cdot10^{-6}$	$2.15\cdot10^{-7}$	$1.14\cdot10^{-16}$
0.5	$3.02\cdot10^{-6}$	$4.32\cdot10^{-7}$	$2.39\cdot10^{-15}$
1	$9.31\cdot10^{-7}$	$5.62\cdot10^{-8}$	$5.55\cdot10^{-15}$
2	$5.00\cdot10^{-7}$	$3.92\cdot10^{-8}$	$7.99\cdot10^{-15}$
3	$8.10\cdot10^{-7}$	$1.50\cdot10^{-7}$	$5.33\cdot10^{-15}$
4	$7.69\cdot10^{-7}$	$1.15\cdot10^{-7}$	$2.66\cdot10^{-15}$
5	$6.64\cdot10^{-7}$	$1.00\cdot10^{-8}$	$8.88\cdot10^{-16}$
6	$5.48\cdot10^{-7}$	$7.18\cdot10^{-8}$	$8.44\cdot10^{-14}$
7	$1.70\cdot10^{-7}$	$7.51\cdot10^{-8}$	$1.19\cdot10^{-12}$
8	$1.09\cdot10^{-7}$	$1.48\cdot10^{-8}$	$1.09\cdot10^{-12}$
9	$1.21\cdot10^{-5}$	$6.85\cdot10^{-8}$	$5.60\cdot10^{-11}$
10	$3.83\cdot10^{-5}$	$1.90\cdot10^{-9}$	$5.66\cdot10^{-11}$



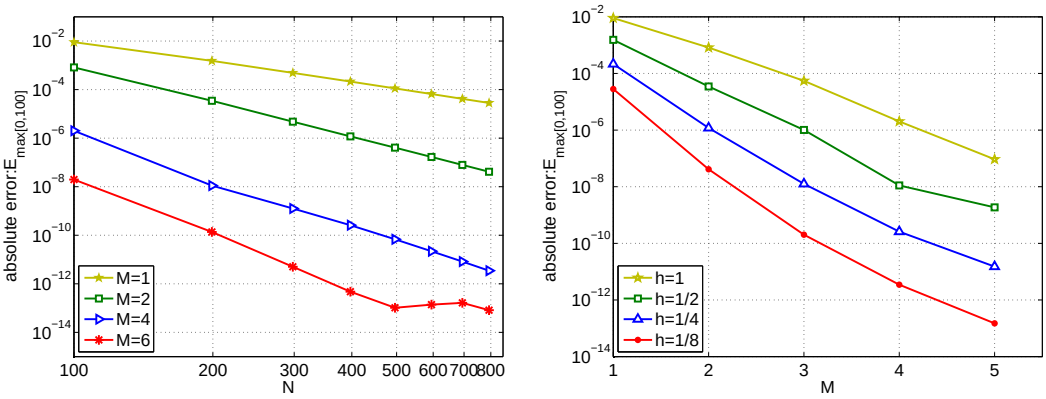
(a) h-version: $T=10$. (b) p-version: $T=10$.

Figure 1: The $E_{\max[0,10]}$ vs $N=T/h$ and the degree of polynomials M for Example 5.1 with $T=10$.

Next, we use Algorithm 2 ($T_0=1$) to solve (5.1) with $t\in[0,100]$. Fig. 2(a) shows the $E_{max[0,100]}$ against N at a fixed uniform mode $M=1,2,4,6$, while Fig. 2(b) shows the $E_{max[0,100]}$ against M with fixed time step sizes $h=1,1/2,1/4,1/8$. From all these numerical results, we can observe the similar convergence phenomenon as for Algorithm 1 mentioned above.

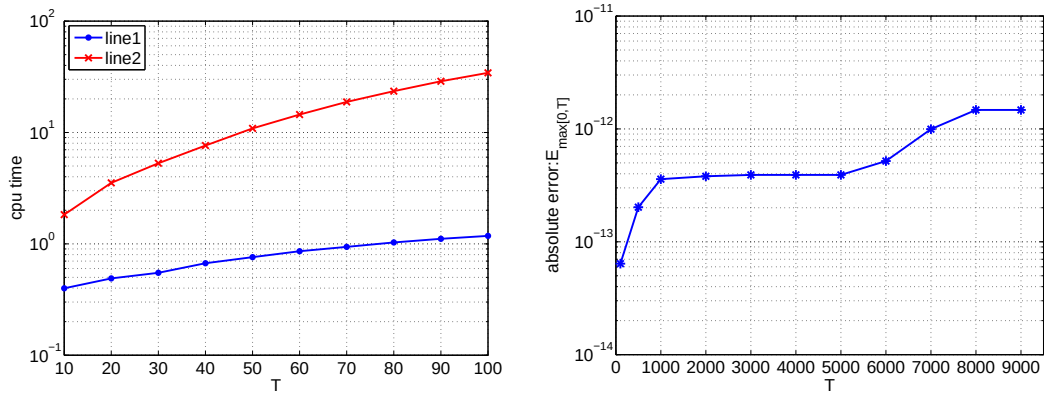
Fig. 3(a) gives the cpu time consumption comparison of Algorithm 1 and Algorithm 2 for Example 5.1. Line 1 shows the cpu time used for various T by Algorithm 2 with $T_0=1$, $h=1/2$, $M=10$ and line 2 shows the corresponding cpu time used by Algorithm

https://doi.org/10.4208/cicp.OA-2016-0181 Published online by Cambridge University Press



(a) h-version: $T=100$. (b) p-version: $T=100$.

Figure 2: The $E_{\max[0,100]}$ vs $N=T/h$ and the degree of polynomials M for Example 5.1 with $T=100$.



(a) Comparison of the time consumption for Algorithms 1 and 2 (b) The $E_{\max[0,T]}$ by Algorithm 2

Figure 3: Long-term simulation for Example 5.1.

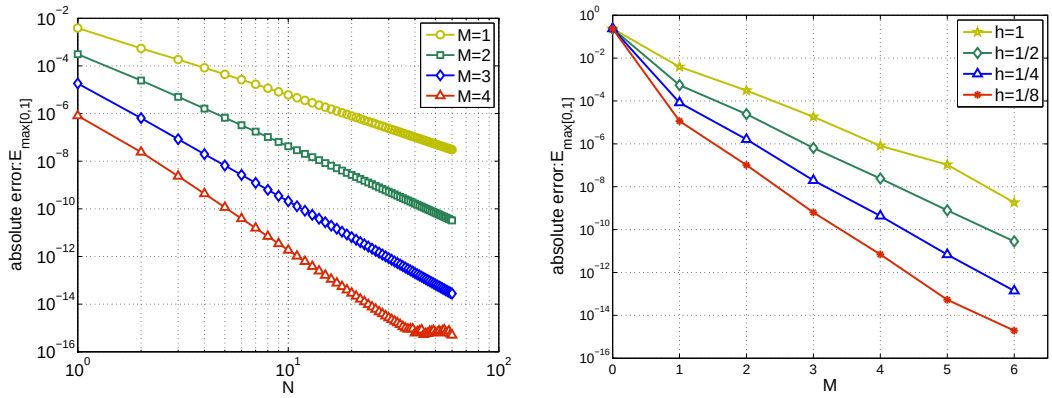
1 with the same h and M, from which we may see that Algorithm 2 requires much less computation cost than Algorithm 1 in long-term simulation. The numerical results by Algorithm 2 are shown in Fig. 3(b), which indicate that this algorithm can produce very accurate solution in long-term simulation as well.

Example 5.2. Consider the thermionic currents equations

$$\begin{cases} u''(t)+\dfrac{a}{t}u'=e^{-u}, \quad t>0, \\ u(0)=0, \quad u'(0)=0. \end{cases} \tag{5.2}$$

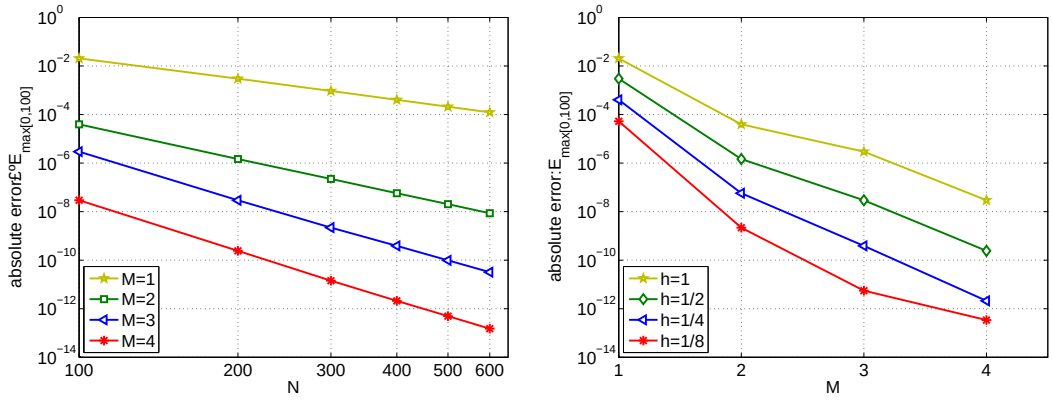
This equation can be used to model the density and electric force of an electron gas in the

https://doi.org/10.4208/cicp.OA-2016-0181 Published online by Cambridge University Press



(a) h-version: $T=1$. (b) p-version: $T=1$.

Figure 4: The $E_{\max[0,1]}$ vs $N=T/h$ and the degree of polynomials M for Example 5.2 with $T=1$.



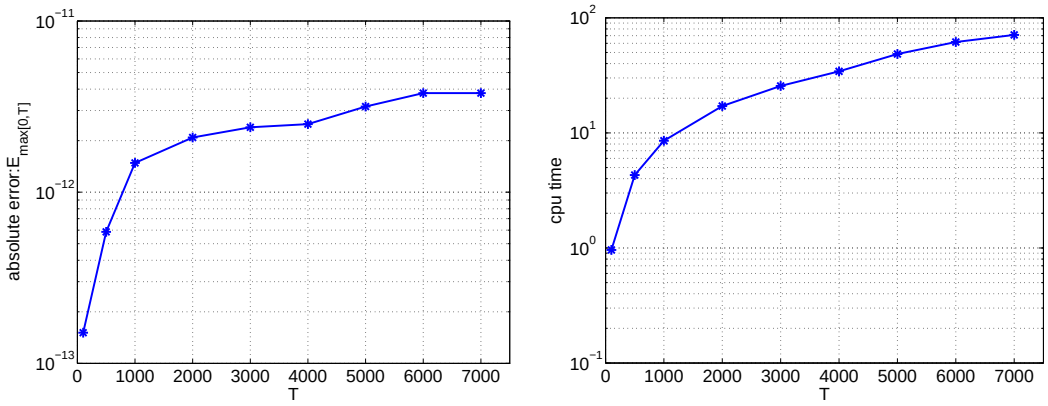
(a) h-version: $T=100$. (b) p-version: $T=100$.

Figure 5: The $E_{\max[0,1]}$ vs $N=T/h$ and the degree of polynomials M for Example 5.2 with $T=100$.

neighborhood of a hot body in thermal equilibrium [17]. In general case, it does not have closed-form solutions. Fortunately, it has an explicit solution for $a=1$: $u=2\ln(1+\frac{t^2}{8})$.

We use Algorithm 1 and Algorithm 2 ($T_0=1$) to numerically solve the problem (5.2), respectively. In Fig. 4(a)/5(a), we show the variation of errors $E_{\max[0,1]}/E_{\max[0,100]}$ over the number of steps N, at a fixed uniform mode $M=1,2,3,4$. The numerical results indicate that the errors decay algebraically with refined time partitions. In Fig. 4(b)/5(b), we plot the errors $E_{\max[0,1]}/E_{\max[0,100]}$ with the variation of M and the fixed time step $h=1,1/2,1/4,1/8$. We observe that the numerical errors decay exponentially as M increases. All these numerical results coincide with the theoretical estimates given in Section 4. Moreover, comparing Fig. 4(a) with Fig. 5(a) and Fig. 4(b) with Fig. 5(b), we may find that

https://doi.org/10.4208/cicp.OA-2016-0181 Published online by Cambridge University Press



(a) The $E_{\max[0,T]}$ for Example 5.2 (b) The time consumption for Example 5.2

Figure 6: The $E_{\max[0,T]}$ and the time consumption for Example 5.2.

compared with Algorithm 1, Algorithm 2 requires fewer collocation points and bigger step sizes to achieve the solution with desired accuracy.

Next, we use Algorithm 2 ($T_0=1$) to solve (5.2) for long-term simulation. In this case, $h_n=h=1/4$ and $M_n=M=8$. Fig. 6(a) shows the variation of the absolute errors $E_{\max[0,T]}$ over various $T\in[1,7000]$. In Fig. 6(b), we plot the corresponding cpu time, from which we may observe that Algorithm 2 can obtain the high accuracy solution with very small amount of computational cost even for long-term simulation.

Example 5.3. Consider the standard Lane-Emden equations

$$\begin{cases} u''(t)+\dfrac{2}{t}u'+u^m=0, \quad t>0, \\ u(0)=1, \quad u'(0)=0. \end{cases} \tag{5.3}$$

This model describes the thermal behavior of a spherical cloud of gas acting under the mutual attraction of its molecules and subject to the classical laws of thermodynamics [4, 11]. Physicists are usually interested in the case of $m\in[0,5]$. However, there are not any closed-form solutions to the problem (5.3) except for $m=0,1,5$ until now.

Then, let us apply Algorithm 1 to solve (5.3) with $m=0.5,1.5,2,2.5,3$. The numerical solutions (LGR solution) are shown in Fig. 7. Moreover, for comparison, we use three different methods for solving (5.3) with $m=3$, including Algorithm 1, the Hermite function collocation method (HFC) (cf. [14]) as well as the rational Legendre Pseudospectral method (RLP) (cf. [15]). Similar to the other related references, we use the numerical results obtained in [11] for $m=3$ as the exact solution or the reference solution. And list the corresponding absolute errors of the three numerical methods at different time in Table 2, from which we may observe that Algorithm 1 has much better approximation accuracy than the other two methods.

https://doi.org/10.4208/cicp.OA-2016-0181 Published online by Cambridge University Press

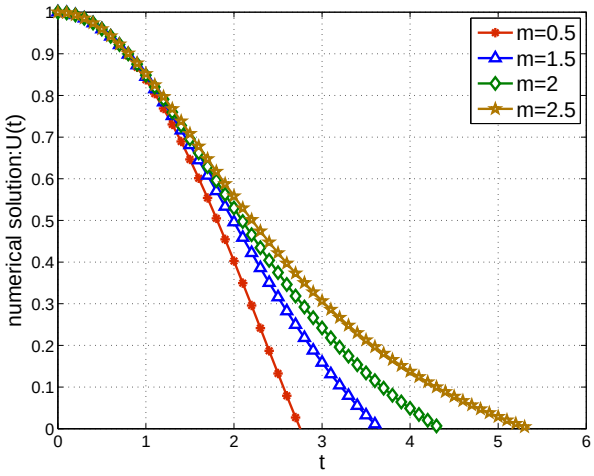


Figure 7: The numerical solutions $U(t)$ for Example 5.3 with different m.

Table 2: Absolute errors of LGR method, HFC method and RLP method for Example 5.3 with $m=3$.

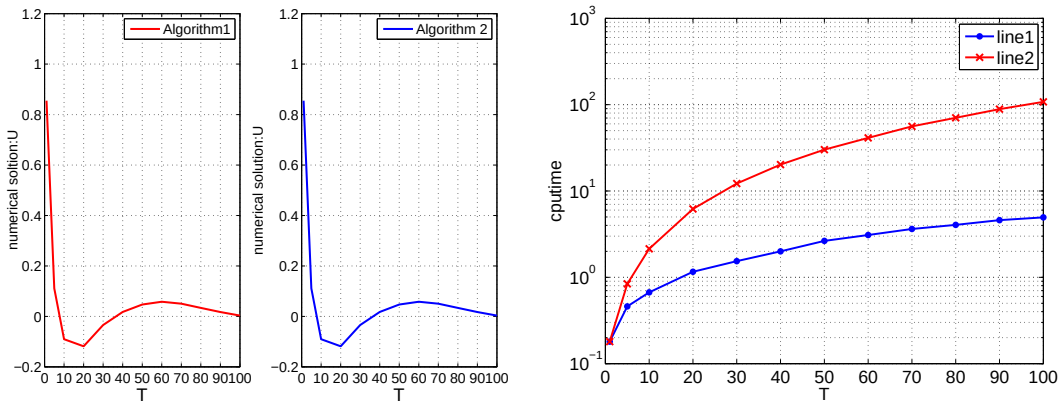
t	LGR-error	HFC-error	RLP-error
0.100	$3.0\cdot10^{-8}$	$1.4\cdot10^{-6}$	$8.1\cdot10^{-7}$
0.500	$3.0\cdot10^{-8}$	$3.0\cdot10^{-6}$	$5.0\cdot10^{-6}$
1.000	$3.1\cdot10^{-8}$	$2.0\cdot10^{-6}$	$1.2\cdot10^{-5}$
5.000	$3.4\cdot10^{-8}$	$3.9\cdot10^{-7}$	$1.1\cdot10^{-5}$
6.000	$2.1\cdot10^{-9}$	$1.1\cdot10^{-6}$	$5.8\cdot10^{-5}$
6.800	$3.6\cdot10^{-10}$	$1.1\cdot10^{-5}$	$1.3\cdot10^{-5}$
6.896	$4.6\cdot10^{-12}$	$9.8\cdot10^{-8}$	$1.3\cdot10^{-7}$

Finally, we solve (5.3) with $m=3$ and $t\in(0,100]$ by Algorithm 1 and Algorithm 2 (T_0=1), respectively. For the two algorithms, we choose h=1/4 and M=5. In Fig. 8(a), we plot the numerical solutions obtained by Algorithm 1 and Algorithm 2. Fig. 8(b) shows the cpu time used for the two algorithms, where Line 1 (resp. 2) indicates the cpu time used by Algorithm 2 (resp. Algorithm 1). From these numerical results, we may observe that Algorithm 2 performs better than Algorithm 1, as shown also in the preceding two numerical examples.

6 Conclusions

The Lane-Emden equation (1.1) frequently occurs in the context of mathematical physics and astrophysics. Due to its importance, a variety of numerical methods were proposed for solving it, among which the spectral method has a significant advantage—it can produce very accurate numerical solution (cf. [19]). However, the spectral methods devel-

https://doi.org/10.4208/cicp.OA-2016-0181 Published online by Cambridge University Press



(a) Numerical solutions (b) Time-consumption

Figure 8: The numerical solutions and the comparison of time consumption for Example 5.3.

oped until now (cf. [5–7, 14]) are not very suitable for long-term computation. In this article, we design a domain decomposition based spectral collocation method for solving the Lane-Emden equation. Essentially, it is a combination of two Legendre-Gauss-Radau collocation schemes for second order differential equations. The first one is a collocation method based on the equivalent Volterra integro-differential equation of (1.1) (cf. (1.2)). Noting that this method is very time-consuming, we next propose a domain decomposition based Legendre-Gauss-Radau spectral collocation method. The idea behind the method is very simple and natural. Since the coefficient function a/t in the equation (1.1) has singularity, we still use the previous method for discretization around $t=0$. After the time T_0, which is a given number as desired, we turn to use the standard multi-step Legendre-Gauss-Radau collocation method for solving the second order differential equation (1.1). After careful and detailed reasoning, it is shown that the errors of both methods have spectral accuracy. Moreover, the latter method require much less computational cost than the foregoing one. We provide a series of numerical experiments to show the numerical performance of the proposed methods (Algorithm 1 and Algorithm 2), which demonstrate that the domain decomposition based method (i.e. Algorithm 2) is particularly suitable for long-term simulation. Compared with the existing methods, Algorithm 2 requires much less computation cost while achieves high-accuracy numerical solution.

Acknowledgments

The authors would like to thank the three referees for their valuable comments and suggestions leading to great improvement of an early version of this article. This work was partially supported by NSFC (Grant No. 11571237).

https://doi.org/10.4208/cicp.OA-2016-0181 Published online by Cambridge University Press

A Appendix

In this appendix, we are going to present the proofs of Theorems 4.1 and 4.2, respectively. To this end, we first recall two well-known lemmas frequently used later on. The first lemma collects some estimates for the Lagrange interpolation operator $\mathcal{I}_{t,M_n}$ (cf. (5.4.33) and (5.4.34) of [3]):

Lemma A.1. *For any $v\in H^r(I_n)$, with integers $1\le r\le M_n+1$, there hold*

$$\|v-\mathcal{I}_{t,M_n}v\|_{I_n}\le cM_n^{-r}h_n^r\|\partial_t^r v\|_{I_n}, \tag{A.1}$$

and

$$\|\partial_t^l\big(v-\mathcal{I}_{t,M_n}v\big)\|_{I_n}\le ch_n^{r-l}M_n^{2l-\frac{1}{2}-r}\|\partial_t^r v\|_{I_n},\quad 1\le l\le r, \tag{A.2}$$

where and in what follows, we simply write $\|\cdot\|_{I_n}$ for $\|\cdot\|_{L^2(I_n)}$.

As given in [20], we have the following Gronwall's inequality:

Lemma A.2. *Assume that $\{k_j\}$ and $\{\rho_j\}$ $(j\ge 0)$ are two given non-negative sequences, and the sequence $\{\varepsilon_n\}$ satisfies $\varepsilon_0\le\rho_0$ and*

$$\varepsilon_n\le\rho_n+\sum_{j=0}^{n-1}q_j+\sum_{j=0}^{n-1}k_j\varepsilon_j,\quad n\ge 1,$$

with $q_j\ge 0$ for $j\ge 0$. Then

$$\varepsilon_n\le\rho_n+\sum_{j=0}^{n-1}(q_j+k_j\rho_j)\exp\Big(\sum_{j=0}^{n-1}k_j\Big),\quad n\ge 1.$$

A.1 The proof for Theorem 4.1

In order to present the proof of Theorem 4.1 more clear, we first derive the following lemma:

Lemma A.3. *Let $G(t,x)$ be a continuous function satisfying the following Lipschitz condition: there exists a positive constant K, independent of t, such that*

$$|G(t,x_1)-G(t,x_2)|\le K|x_1-x_2|,\quad \forall x_1,x_2\in\mathbb{R}. \tag{A.3}$$

Then, for any $n\ge 1$ there holds

$$\|\mathcal{I}_{t,M_n}(G(t,\psi)-G(t,\Psi))\|_{I_n}\le c_1K\|\mathcal{I}_{t,M_n}\psi-\Psi\|_{I_n},\quad \forall\psi\in C(I_n),\Psi\in P_{M_n+1}(I_n),$$

where $c_1=\sqrt{2+\frac{2}{2M_n+1}}$.

https://doi.org/10.4208/cicp.OA-2016-0181 Published online by Cambridge University Press

Proof. By virtue of (2.7), we have

$$\int_{I_n}\left(\mathcal{I}_{t,M_n}(G(t,\psi)-G(t,\Psi))\right)^2 ds=\frac{h_n}{2}\sum_{i=0}^{M_n}(G(t_{n,i},\psi(t_{n,i}))-G(t_{n,i},\Psi(t_{n,i})))^2\omega_{n,i}=:\mathrm{I}. \quad (A.4)$$

On the other hand, it follows from (A.3) and Lemma 2.1 of [25] that

$$\begin{aligned}\mathrm{I}&\le\frac{h_n}{2}\sum_{i=0}^{M_n}K^2(\psi(t_{n,i})-\Psi(t_{n,i}))^2\omega_{n,i}\\&=K^2\int_{I_n}\left(\mathcal{I}_{t,M_n}(\psi(t)-\Psi(t))\right)^2 ds\le c_1^2K^2\|\mathcal{I}_{t,M_n}\psi-\Psi\|_{I_n}^2,\end{aligned}$$

from which and (A.4) the required result follows readily. □

Now, we proceed with the error analysis for Algorithm 1 on each subinterval I_n. According to (3.1),

$$\mathcal{I}_{t,M_n}\Big[\frac{d}{dt}(u_n(t))+\sum_{k=1}^{n-1}\int_{I_k}\frac{s^a}{t^a}f(u_k)ds+\frac{t-t_{n-1}}{h_n}\int_{I_n}\frac{[\sigma(\lambda,t)]^a}{t^a}f(u_n(\sigma(\lambda,t)))d\lambda\Big]=0. \quad (A.5)$$

Let

$$\begin{aligned}&E_n(t):=u_n(t)-U_n(t),\\&B_1(t):=\mathcal{I}_{t,M_n}\Big(\frac{d}{dt}u_n(t)\Big)-\frac{d}{dt}u_n(t),\\&B_{2,k}(t):=\mathcal{I}_{t,M_n}\int_{I_k}\Big(\mathcal{I}-\mathcal{I}_{s,M_k}\Big)\Big(\frac{s^a}{t^a}f(u_k)\Big)ds,\\&B_{3,k}(t):=\mathcal{I}_{t,M_n}\int_{I_k}\mathcal{I}_{s,M_k}\Big(\frac{s^a}{t^a}f(u_k)-\frac{s^a}{t^a}f(U_k)\Big)ds,\\&B_4(t):=\mathcal{I}_{t,M_n}\frac{t-t_{n-1}}{h_n}\int_{I_n}\Big(\mathcal{I}-\mathcal{I}_{\lambda,M_n}\Big)\Big(\frac{[\sigma(\lambda,t)]^a}{t^a}f(u_n(\sigma(\lambda,t))\Big)d\lambda,\\&B_5(t):=\mathcal{I}_{t,M_n}\frac{t-t_{n-1}}{h_n}\int_{I_n}\mathcal{I}_{\lambda,M_n}\Big(\frac{[\sigma(\lambda,t)]^a}{t^a}\big[f(u_n(\sigma(\lambda,t)))-f(U_n(\sigma(\lambda,t)))\big]\Big)d\lambda.\end{aligned} \quad (A.6)$$

Subtracting (3.3) from (A.5) yields

$$E_n'(t)+B_1(t)+\sum_{k=1}^{n-1}B_{2,k}(t)+\sum_{k=1}^{n-1}B_{3,k}(t)+B_4(t)+B_5(t)=0,\quad t\in I_n. \quad (A.7)$$

Next, we estimate $\|B_1\|_{I_n}$. Clearly, from (A.1) it follows that

$$\|B_1\|_{I_n}^2=\|\mathcal{I}_{t,M_n}\Big(\frac{d}{dt}u_n(t)\Big)-\frac{d}{dt}u_n(t)\|_{I_n}^2\le cM_n^{2-2r}h_n^{2r-2}\|\partial_t^r u_n\|_{I_n}^2. \quad (A.8)$$

https://doi.org/10.4208/cicp.OA-2016-0181 Published online by Cambridge University Press

Using (2.7), (A.1) and (A.6), we have

$$\begin{aligned}\|B_{2,k}\|_{I_n}^2 &= \frac{h_n}{2}\sum_{i=0}^{M_n}\Big(\int_{I_k}(\mathcal{I}-\mathcal{I}_{s,M_k})\big(\frac{s^a}{t_{n,i}^a}f(u_k)\big)ds\Big)^2\omega_{n,i}\\ &\le \frac{h_n}{2}\sum_{i=0}^{M_n}cM_k^{-2r}h_k^{2r+1}\int_{I_k}\Big(\partial_s^r\big(\frac{s^a}{t_{n,i}^a}f(u_k)\big)\Big)^2ds\cdot\omega_{n,i}\\ &\le \frac{h_n}{2}\sum_{i=0}^{M_n}cM_k^{-2r}h_k^{2r+1-2a}\|f(u_k(\cdot))\|_{H^r(I_k)}^2\cdot\omega_{n,i}\\ &\le cM_k^{-2r}h_k^{2r+1-2a}h_n\|f(u_k(\cdot))\|_{H^r(I_k)}^2.\end{aligned}\tag{A.9}$$

Using (2.7), (4.1) and Lemma A.3, we have

$$\begin{aligned}\|B_{3,k}\|_{I_n}^2 &= \frac{h_n}{2}\sum_{i=0}^{M_n}\Big(\int_{I_k}\mathcal{I}_{s,M_k}\Big(\frac{s^a}{t_{n,i}^a}f(u_k)-\frac{s^a}{t_{n,i}^a}f(U_k)\Big)ds\Big)^2\omega_{n,i}\\ &\le \frac{h_n}{2}\sum_{i=0}^{M_n}h_k\int_{I_k}\Big(\mathcal{I}_{s,M_k}\big(\frac{s^a}{t_{n,i}^a}f(u_k)-\frac{s^a}{t_{n,i}^a}f(U_k)\big)\Big)^2ds\cdot\omega_{n,i}\\ &\le c_1^2L^2h_nh_k\|\mathcal{I}_{s,M_k}u_k-U_k\|_{I_k}^2.\end{aligned}\tag{A.10}$$

Furthermore, we have by (A.1) and (A.10) that

$$\begin{aligned}\|B_{3,k}\|_{I_n}^2 &\le 2c_1^2L^2h_nh_k\big(\|\mathcal{I}_{s,M_k}u_k-u_k\|_{I_k}^2+\|u_k-U_k\|_{I_k}^2\big)\\ &\le cL^2h_nh_k^{2r+1}M_k^{-2r}\|\partial_t^ru_k\|_{I_k}^2+2c_1^2L^2h_nh_k\|E_k\|_{I_k}^2.\end{aligned}\tag{A.11}$$

Similarly, according to (2.7) and (A.1),

$$\begin{aligned}\|B_4\|_{I_n}^2 &= \frac{h_n}{2}\sum_{i=0}^{M_n}\Big[\frac{t_{n,i}-t_{n-1}}{h_n}\int_{I_n}\Big(\mathcal{I}-\mathcal{I}_{\lambda,M_n}\Big)\Big(\frac{[\sigma(\lambda,t_{n,i})]^a}{t^a}f(u_n(\sigma(\lambda,t_{n,i})))\Big)d\lambda\Big]^2\omega_{n,i}\\ &\le cM_n^{-2r}h_n^{2r+2}\sum_{i=0}^{M_n}\Big(\frac{t_{n,i}-t_{n-1}}{h_n}\Big)^2\int_{I_n}\Big[\partial_\lambda^r\Big(\frac{[\sigma(\lambda,t_{n,i})]^a}{t^a}f(u_n(\sigma(\lambda,t_{n,i})))\Big)\Big]^2d\lambda\cdot\omega_{n,i}\\ &\le cM_n^{-2r}h_n^{2r+2-2a}\sum_{i=0}^{M_n}\|f(u_n(\cdot))\|_{H^r(I_n)}^2\cdot\omega_{n,i}\le cM_n^{-2r}h_n^{2r+2-2a}\|f(u_n(\cdot))\|_{H^r(I_n)}^2.\end{aligned}\tag{A.12}$$

Finally, we estimate $\|B_5\|_{I_n}^2$. From (2.7), (4.1), (A.1) and Lemma A.3, it follows that

$$\begin{aligned}&\|B_5\|_{I_n}^2\\ &=\frac{h_n}{2}\sum_{i=0}^{M_n}\Big(\frac{t_{n,i}-t_{n-1}}{h_n}\Big)^2\Big[\int_{I_n}\mathcal{I}_{\lambda,M_n}\Big(\frac{\sigma(\lambda,t_{n,i})^a}{t_{n,i}^a}\big(f(u_n(\sigma(\lambda,t_{n,i})))-f(U_n(\sigma(\lambda,t_{n,i})))\big)\Big)d\lambda\Big]^2\omega_{n,i}\end{aligned}$$

https://doi.org/10.4208/cicp.OA-2016-0181 Published online by Cambridge University Press

$$\leq\frac{(c_1h_n)^2}{2}L^2\sum_{i=0}^{M_n}\Big(\frac{t_{n,i}-t_{n-1}}{h_n}\Big)^2\int_{I_n}\big(\mathcal{I}_{\lambda,M_n}u_n(\sigma(\lambda,t_{n,i}))-U_n(\sigma(\lambda,t_{n,i}))\big)^2d\lambda\cdot\omega_{n,i}$$
$$\leq cM_n^{-2r}h_n^{2r+2}L^2\sum_{i=0}^{M_n}\Big(\frac{t_{n,i}-t_{n-1}}{h_n}\Big)^2\int_{I_n}\big(\partial_\lambda^r u_n(\sigma(\lambda,t_{n,i}))\big)^2d\lambda\cdot\omega_{n,i}$$
$$+(c_1h_n)^2L^2\sum_{i=0}^{M_n}\Big(\frac{t_{n,i}-t_{n-1}}{h_n}\Big)\int_{I_n}\big(u_n(s)-U_n(s)\big)^2ds\cdot\omega_{n,i}. \tag{A.13}$$

On the other hand, by the chain rule for differentiation, we find

$$\int_{I_n}\big(\partial_\lambda^r u_n(\sigma(\lambda,t_{n,i}))\big)^2d\lambda=\Big(\frac{t_{n,i}-t_{n-1}}{h_n}\Big)^{2r-1}\int_{t_{n-1}}^{t_{n,i}}\big(\partial_s^r u_n(s)\big)^2ds,$$

which combined with (A.13) gives

$$\|B_5\|_{I_n}^2\leq cM_n^{-2r}h_n^{2r+2}L^2\sum_{i=0}^{M_n}\Big(\frac{t_{n,i}-t_{n-1}}{h_n}\Big)^{2r+1}\int_{t_{n-1}}^{t_{n,i}}\big(\partial_s^r u_n(s)\big)^2ds\cdot\omega_{n,i}$$
$$+(c_1h_n)^2L^2\sum_{i=0}^{M_n}\Big(\frac{t_{n,i}-t_{n-1}}{h_n}\Big)\int_{I_n}\big(u_n(s)-U_n(s)\big)^2ds\cdot\omega_{n,i}$$
$$\leq cM_n^{-2r}h_n^{2r+2}L^2\|\partial_s^r u_n\|_{I_n}^2+(c_1h_n)^2L^2\|E_n\|_{I_n}^2. \tag{A.14}$$

Moreover, thanks to (A.7) and the Cauchy-Schwarz inequality, we know

$$\|E_n'\|_{I_n}^2\leq 5\Big[\|B_1\|_{I_n}^2+\|\sum_{k=1}^{n-1}B_{2,k}h_k^{1/2}\cdot h_k^{-1/2}\|_{I_n}^2+\|\sum_{k=1}^{n-1}B_{3,k}h_k^{1/2}\cdot h_k^{-1/2}\|_{I_n}^2+\|B_4\|_{I_n}^2+\|B_5\|_{I_n}^2\Big]$$
$$\leq 5\Big[\|B_1\|_{I_n}^2+T\sum_{k=1}^{n-1}h_k^{-1}\|B_{2,k}\|_{I_n}^2+T\sum_{k=1}^{n-1}h_k^{-1}\|B_{3,k}\|_{I_n}^2+\|B_4\|_{I_n}^2+\|B_5\|_{I_n}^2\Big],$$

which, in conjunction with (A.8)-(A.14), leads to

$$\|E_n'\|_{I_n}^2\leq cM_n^{2-2r}h_n^{2r-2}\|\partial_t^r u_n\|_{I_n}^2+cT\sum_{k=1}^{n-1}M_k^{-2r}h_k^{2r-2a}h_n\|f(u_k(\cdot))\|_{H^r(I_k)}^2$$
$$+cT\sum_{k=1}^{n-1}L^2h_nh_k^{2r}M_k^{-2r}\|\partial_t^r u_k\|_{I_k}^2+cT\sum_{k=1}^{n-1}L^2h_n\|E_k\|_{I_k}^2$$
$$+cM_n^{-2r}h_n^{2r+2-2a}\|f(u_n(\cdot))\|_{H^r(I_n)}^2+5(c_1h_n)^2L^2\|E_n\|_{I_n}^2. \tag{A.15}$$

On the other hand, it is evident that

$$\begin{cases}E_k^2(t_k)-E_k^2(t_{k-1})=2\displaystyle\int_{I_k}E_k'(t)E_k(t)dt\leq\|E_k\|_{H^1(I_k)}^2,\\ E_k(t_{k-1})=E_{k-1}(t_{k-1}),\qquad E_1(t_0)=0.\end{cases}$$

https://doi.org/10.4208/cicp.OA-2016-0181 Published online by Cambridge University Press

Summing up all these inequalities, we obtain

$$E_{n-1}^2(t_{n-1}) \le \sum_{k=1}^{n-1} \|E_k\|_{H^1(I_k)}^2. \tag{A.16}$$

Therefore,

$$\begin{aligned}\|E_n\|_{I_n}^2 &= \int_{I_n} \Big(\int_{t_{n-1}}^t E_n'(s)ds + E_n(t_{n-1}) \Big)^2 dt \le 2h_n^2 \|E_n'\|_{I_n}^2 + 2h_n E_n^2(t_{n-1}) \\ &= 2h_n^2 \|E_n'\|_{I_n}^2 + 2h_n E_{n-1}^2(t_{n-1}) \le 2h_n^2 \|E_n'\|_{I_n}^2 + 2h_n \sum_{k=1}^{n-1} \|E_k\|_{H^1(I_k)}^2.\end{aligned}$$

This along with (A.15) yields

$$\begin{aligned}\|E_n\|_{H^1(I_n)}^2 \le{}& cM_n^{2-2r} h_n^{2r-2} \|\partial_t^r u_n\|_{I_n}^2 + cT \sum_{k=1}^{n-1} M_k^{-2r} h_k^{2r-2a} h_n \|f(u_k(\cdot))\|_{H^r(I_k)}^2 \\ &+ cT \sum_{k=1}^{n-1} L^2 h_n h_k^{2r} M_k^{-2r} \|\partial_t^r u_k\|_{I_k}^2 + cT \sum_{k=1}^{n-1} L^2 h_n \|E_k\|_{H^1(I_k)}^2 \\ &+ cM_n^{-2r} h_n^{2r+2-2a} \|f(u_n(\cdot))\|_{H^r(I_n)}^2 + 5(c_1 h_n)^2 L^2 \|E_n\|_{I_n}^2 + 2h_n^2 \|E_n'\|_{I_n}^2. \end{aligned} \tag{A.17}$$

If

$$\max\left(5c_1^2 h_n^2 L^2,\, 2h_n^2\right) \le \eta < 1, \tag{A.18}$$

then we may rewrite (A.17) as

$$\|E_n\|_{H^1(I_n)}^2 \le cT \sum_{k=1}^{n-1} L^2 h_n \|E_k\|_{H^1(I_k)}^2 + Q_n, \tag{A.19}$$

where

$$\begin{aligned}Q_n ={}& cT \sum_{k=1}^{n-1} \left(M_k^{-2r} h_k^{2r-2a} h_n \|f(u_k(\cdot))\|_{H^r(I_k)}^2 + L^2 h_n h_k^{2r} M_k^{-2r} \|\partial_t^r u_k\|_{I_k}^2 \right) \\ &+ cM_n^{2-2r} h_n^{2r-2} \|\partial_t^r u_n\|_{I_n}^2 + cM_n^{-2r} h_n^{2r+2-2a} \|f(u_n(\cdot))\|_{H^r(I_n)}^2.\end{aligned}$$

By taking $\varepsilon_k = h_k^{-1} \|E_k\|_{H^1(I_k)}^2$ in Lemma A.2, we can get from (A.19) that

$$\begin{aligned}&\|u_n - U_n\|_{H^1(I_n)}^2 = \|E_n\|_{H^1(I_n)}^2 \\ &\le \exp(cT^2L^2) h_n \sum_{k=1}^{n-1} \left[M_k^{2-2r} h_k^{2r-2} \|\partial_t^r u_k\|_{I_k}^2 + TM_k^{-2r} h_k^{2r-2a} \|f(u_k(\cdot))\|_{H^r(I_k)}^2 \right] \\ &+ cM_n^{2-2r} h_n^{2r-2} \|\partial_t^r u_n\|_{I_n}^2 + cM_n^{-2r} h_n^{2r+2-2a} \|f(u_n(\cdot))\|_{H^r(I_n)}^2. \end{aligned} \tag{A.20}$$

https://doi.org/10.4208/cicp.OA-2016-0181 Published online by Cambridge University Press

Furthermore, by setting $T=t_N$, we have from (A.20) that

$$\begin{aligned}&\|u-U\|^2_{H^1(0,T)}\\ \le&\exp(cT^2L^2)\sum_{n=1}^{N}\Big[h_n\sum_{k=1}^{n-1}\big[M_k^{2-2r}h_k^{2r-2}\|\partial_t^r u_k\|^2_{I_k}+TM_k^{-2r}h_k^{2r-2a}\|f(u_k(\cdot))\|^2_{H^r(I_k)}\big]\\ &+M_n^{2-2r}h_n^{2r-2}\|\partial_t^r u_n\|^2_{I_n}+M_n^{-2r}h_n^{2r+2-2a}\|f(u_n(\cdot))\|^2_{H^r(I_n)}\Big].\end{aligned}$$

Let $h:=\max_{1\le n\le N_T}h_n$ and $M:=\min_{1\le n\le N_T}M_n$. Then the above estimate can be simply rewritten as

$$\begin{aligned}&\|u-U\|^2_{H^1(0,T)}\\ \le&\exp(cT^2L^2)\big[TM^{2-2r}h^{2r-2}\|\partial_t^r u\|^2_{L^2(0,T)}+T^2M^{-2r}h^{2r-2a}\|f(u(\cdot))\|^2_{H^r(0,T)}\big].\end{aligned}\tag{A.21}$$

With the aid of (A.16) and (A.21), we also have

$$\begin{aligned}&|u(T)-U(T)|^2\\ \le&\exp(cT^2L^2)\big[TM^{2-2r}h^{2r-2}\|\partial_t^r u\|^2_{L^2(0,T)}+T^2M^{-2r}h^{2r-2a}\|f(u(\cdot))\|^2_{H^r(0,T)}\big].\end{aligned}$$

In addition, we have by (3.1) and (3.3) that

$$|u'(T)-U'(T)|^2=\Big|\sum_{k=1}^{N}\int_{I_k}\Big(\frac{s^a}{T^a}f(s,u_k)-\mathcal{I}_{s,M_k}\frac{s^a}{T^a}f(s,U_k)ds\Big)\Big|^2.$$

This along with Lemma A.3 and the Cauchy-Schwarz inequality gives

$$\begin{aligned}|u'(T)-U'(T)|^2&\le T\sum_{k=1}^{N}\int_{I_k}\Big(\frac{s^a}{T^a}f(u_k)-\mathcal{I}_{s,M_k}\frac{s^a}{T^a}f(U_k)\Big)^2ds\\ &\le 2T\sum_{k=1}^{N}\int_{I_k}\Big[\Big((\mathcal{I}-\mathcal{I}_{s,M_k})\frac{s^a}{T^a}f(u_k)\Big)^2+\Big(\mathcal{I}_{s,M_k}\frac{s^a}{T^a}(f(u_k)-f(U_k))\Big)^2\Big]ds.\\ &\le 2T\sum_{k=1}^{N}\Big(\|(\mathcal{I}-\mathcal{I}_{s,M_k})\frac{s^a}{T^a}f(u_k)\|^2_{I_k}+c_1^2L^2\|\mathcal{I}_{s,M_k}u_k-U_k\|^2_{I_k}\Big).\end{aligned}$$

Therefore we use Lemma A.1 and (A.21) successively to deduce that

$$\begin{aligned}&|u'(T)-U'(T)|^2\\ \le&\exp(cT^2L^2)\big[T^2M^{2-2r}h^{2r-2}\|\partial_t^r u\|^2_{L^2(0,T)}+T^3M^{-2r}h^{2r-2a}\|f(u(\cdot))\|^2_{H^r(0,T)}\big].\end{aligned}$$

This completes the proof of Theorem 4.1.

https://doi.org/10.4208/cicp.OA-2016-0181 Published online by Cambridge University Press

A.2 The proof for Theorem 4.2

In this part of appendix, we will establish the error analysis of Theorem 4.2. First of all, it follows from (1.3) that

$$\mathcal{I}_{t,M_n}u_n''(t)+\frac{a}{t}\mathcal{I}_{t,M_n}u_n'+f(\mathcal{I}_{t,M_n}u_n)=0,\quad t\in\{t_{n,j}\}_{j=0}^{M_n}. \tag{A.22}$$

Let

$$\widetilde{E}_n(t):=U_n(t)-\mathcal{I}_{t,M_n}u_n(t),$$
$$G_1^n(t):=\mathcal{I}_{t,M_n}u_n''(t)-\big(\mathcal{I}_{t,M_n}u_n(t)\big)'', \tag{A.23}$$
$$G_2^n(t):=\frac{a}{t}\big(\mathcal{I}_{t,M_n}u_n'-(\mathcal{I}_{t,M_n}u_n)'\big), \tag{A.24}$$
$$G_3^n(t):=\frac{a}{t}\big((\mathcal{I}_{t,M_n}u_n)'-U_n'(t)\big), \tag{A.25}$$
$$G_4^n(t):=f(\mathcal{I}_{t,M_n}u_n)-f(U_n). \tag{A.26}$$

Subtracting (A.22) from (3.17) leads to

$$\widetilde{E}_n''(t)=\sum_{i=1}^{4}G_i^n(t),\quad t\in\{t_{n,j}\}_{j=0}^{M_n},\quad n\geq 1. \tag{A.27}$$

On the other hand, after a direct manipulation, we know

$$\begin{aligned}&((t-t_{n-1})^{-1}(\widetilde{E}_n'(t)-\widetilde{E}_n'(t_{n-1})))'\\ =&-(t-t_{n-1})^{-2}(\widetilde{E}_n'(t)-\widetilde{E}_n'(t_{n-1}))+(t-t_{n-1})^{-1}\widetilde{E}_n''(t),\quad t\in\{t_{n,j}\}_{j=0}^{M_n},\quad n\geq 1.\end{aligned} \tag{A.28}$$

Multiplying (A.28) by $2(\widetilde{E}_n'(t_{n,j})-\widetilde{E}_n'(t_{n-1}))\omega_{n,j}$ and then summing over j with $0\leq j\leq M_n$, we have from (A.27) that

$$\begin{aligned}&2\langle(((t-t_{n-1})^{-1}(\widetilde{E}_n'(t)-\widetilde{E}_n'(t_{n-1})))',\widetilde{E}_n'-\widetilde{E}_n'(t_{n-1})\rangle_{I_n}\\ =&-2\langle(t-t_{n-1})^{-2}(\widetilde{E}_n'-\widetilde{E}_n'(t_{n-1})),\widetilde{E}_n'-\widetilde{E}_n'(t_{n-1})\rangle_{I_n}\\ &+2\Big\langle(t-t_{n-1})^{-1}(\widetilde{E}_n'-\widetilde{E}_n'(t_{n-1})),\sum_{i=1}^{4}G_i^n\Big\rangle_{I_n}.\end{aligned} \tag{A.29}$$

Since $\widetilde{E}_n'(t)-\widetilde{E}_n'(t_{n-1})\in P_{M_n+1}(I_n)$ and $(t-t_{n-1})^{-1}(\widetilde{E}_n'-\widetilde{E}_n'(t_{n-1}))\in P_{M_n}(I_n)$, we have by (2.7) and (A.29) that

$$\begin{aligned}&h_n^{-1}(\widetilde{E}_n'(t_n)-\widetilde{E}_n'(t_{n-1}))^2+\|(t-t_{n-1})^{-1}(\widetilde{E}_n'-\widetilde{E}_n'(t_{n-1}))\|_{I_n}^2\\ =&2\Big\langle(t-t_{n-1})^{-1}(\widetilde{E}_n'-\widetilde{E}_n'(t_{n-1})),\sum_{i=1}^{4}G_i^n\Big\rangle_{I_n}.\end{aligned}$$

https://doi.org/10.4208/cicp.OA-2016-0181 Published online by Cambridge University Press

This implies that

$$h_n^{-1}(\widetilde{E}_n'(t_n)-\widetilde{E}_n'(t_{n-1}))^2\le 2\Big\langle (t-t_{n-1})^{-1}(\widetilde{E}_n'-\widetilde{E}_n'(t_{n-1})),\sum_{i=1}^4 G_i^n\Big\rangle_{I_n},$$

and

$$\|(t-t_{n-1})^{-1}(\widetilde{E}_n'-\widetilde{E}_n'(t_{n-1}))\|_{I_n}^2\le 2\Big\langle (t-t_{n-1})^{-1}(\widetilde{E}_n'-\widetilde{E}_n'(t_{n-1})),\sum_{i=1}^4 G_i^n\Big\rangle_{I_n}.$$

Again, using (2.7) and the Cauchy-Schwarz inequality, we find

$$\|(t-t_{n-1})^{-1}(\widetilde{E}_n'-\widetilde{E}_n'(t_{n-1}))\|_{I_n}\le 2\Big\|\sum_{i=1}^4 G_i^n\Big\|_{I_n,M_n}\le 2\sum_{i=1}^4\|G_i^n\|_{I_n,M_n}, \tag{A.30}$$

and

$$h_n^{-1}(\widetilde{E}_n'(t_n)-\widetilde{E}_n'(t_{n-1}))^2\le 2\Big\|\sum_{i=1}^4 G_i^n\Big\|_{I_n,M_n}\|(t-t_{n-1})^{-1}(\widetilde{E}_n'-\widetilde{E}_n'(t_{n-1}))\|_{I_n}. \tag{A.31}$$

For bounding $\|G_1^n\|_{I_n,M_n}$, we have by (2.7), (A.23) and Lemma A.1 that

$$\begin{aligned}\|G_1^n\|_{I_n,M_n}&=\|G_1^n\|_{I_n}\le\|\mathcal{I}_{t,M_n}u_n''-u_n''\|_{I_n}+\|u_n''-\big(\mathcal{I}_{t,M_n}u_n(t)\big)''\|_{I_n}\\&\le ch_n^{r-2}M_n^{2-r}\|\partial_t^r u_n\|_{I_n}+ch_n^{r-2}M_n^{\frac{7}{2}-r}\|\partial_t^r u_n\|_{I_n}\\&\le ch_n^{r-2}M_n^{\frac{7}{2}-r}\|\partial_t^r u_n\|_{I_n}.\end{aligned} \tag{A.32}$$

Similarly, by (2.7), (A.24) and Lemma A.1,

$$\|G_2^n\|_{I_n,M_n}\le\frac{a}{T_0}\|\mathcal{I}_{t,M_n}u_n'-(\mathcal{I}_{t,M_n}u_n)'\|_{I_n}\le\frac{ca}{T_0}h_n^{r-1}M_n^{\frac{3}{2}-r}\|\partial_t^r u_n\|_{I_n}. \tag{A.33}$$

With the aid of (A.25) and Lemma 2.1 of [25], we obtain

$$\|G_3^n\|_{I_n,M_n}\le\frac{a}{T_0}\|\widetilde{E}_n'\|_{I_n,M_n}\le\frac{c_1a}{T_0}\|\widetilde{E}_n'\|_{I_n}. \tag{A.34}$$

According to (A.26), (4.1) and (3.303a) of [19],

$$\|G_4^n\|_{I_n,M_n}\le L\|\mathcal{I}_{t,M_n}u_n-U_n\|_{I_n,M_n}\le c_2L\|\widetilde{E}_n\|_{I_n}, \tag{A.35}$$

where the generic constant c_2 is proportional to $2+\frac{2}{M_n}$. Therefore, we have by (A.32)-(A.35) and (A.27) that

$$\|\widetilde{E}_n''\|_{I_n}\le ch_n^{r-2}M_n^{7/2-r}\|\partial_t^r u_n\|_{I_n}+c_2L\|\widetilde{E}_n\|_{I_n}+\frac{c_1a}{T_0}\|\widetilde{E}_n'\|_{I_n}. \tag{A.36}$$

https://doi.org/10.4208/cicp.OA-2016-0181 Published online by Cambridge University Press

In addition, the combination of (A.30)-(A.35) yields

$$\|(\widetilde{E}_n'-\widetilde{E}_n'(t_{n-1}))\|_{I_n}\leq ch_n^{r-1}M_n^{\frac{7}{2}-r}\|\partial_t^r u_n\|_{I_n}+2c_2h_nL\|\widetilde{E}_n\|_{I_n}+\frac{2c_1a}{T_0}h_n\|\widetilde{E}_n'\|_{I_n},$$

which along with the triangle inequality leads to

$$\|\widetilde{E}_n'\|_{I_n}\leq ch_n^{r-1}M_n^{\frac{7}{2}-r}\|\partial_t^r u_n\|_{I_n}+2c_2h_nL\|\widetilde{E}_n\|_{I_n}+\frac{2c_1a}{T_0}h_n\|\widetilde{E}_n'\|_{I_n}+h_n^{\frac{1}{2}}|\widetilde{E}_n'(t_{n-1}))|. \tag{A.37}$$

If

$$d_1:=1-\frac{2c_1a}{T_0}h_n\geq d>0,$$

we can conclude from (A.37) that

$$\|\widetilde{E}_n'\|_{I_n}\leq ch_n^{r-1}M_n^{\frac{7}{2}-r}\|\partial_t^r u_n\|_{I_n}+\frac{2c_2h_nL}{d_1}\|\widetilde{E}_n\|_{I_n}+ch_n^{\frac{1}{2}}|\widetilde{E}_n'(t_{n-1}))|. \tag{A.38}$$

On the other hand, by the Poincaré inequality,

$$\|\widetilde{E}_n\|_{I_n}\leq\sqrt{2}h_n^{\frac{1}{2}}|\widetilde{E}_n(t_{n-1}))|+2h_n\|\widetilde{E}_n'\|_{I_n},$$

and with (A.38) we further have

$$\|\widetilde{E}_n\|_{I_n}\leq ch_n^{r}M_n^{\frac{7}{2}-r}\|\partial_t^r u_n\|_{I_n}+\frac{4c_2h_n^2L}{d1}\|\widetilde{E}_n\|_{I_n}+ch_n^{\frac{3}{2}}|\widetilde{E}_n'(t_{n-1}))|+\sqrt{2}h_n^{\frac{1}{2}}|\widetilde{E}_n(t_{n-1}))|. \tag{A.39}$$

Therefore, if

$$d_0:=1-\frac{4c_2h_n^2L}{d1}\geq d>0, \tag{A.40}$$

then we have from (A.39) that

$$\|\widetilde{E}_n\|_{I_n}\leq ch_n^{r}M_n^{\frac{7}{2}-r}\|\partial_t^r u_n\|_{I_n}+ch_n^{\frac{3}{2}}|\widetilde{E}_n'(t_{n-1}))|+ch_n^{\frac{1}{2}}|\widetilde{E}_n(t_{n-1}))|. \tag{A.41}$$

Now, it remains to bound $|\widetilde{E}_n(t_{n-1})|$ and $|\widetilde{E}_n'(t_{n-1})|$ for $n\geq N+1$. We first consider the case of $n=N+1$. Since for any $v\in H^1(I_n)$ (see page 279 of [9]),

$$|v(t)|^2\leq h_n^{-1}\|v\|_{I_n}^2+h_n\|\partial_t v\|_{I_n}^2, \tag{A.42}$$

which along with Lemma A.1 implies

$$\begin{aligned}
&|\widetilde{E}_{N+1}(t_N)|=|U_{N+1}(t_N)-\mathcal{I}_{t,M_{N+1}}u_{N+1}(t_N)|\\
\leq& h_{N+1}^{-\frac{1}{2}}\|u_{N+1}-\mathcal{I}_{t,M_{N+1}}u_{N+1}\|_{I_{N+1}}+h_{N+1}^{\frac{1}{2}}\|\partial_t(u_{N+1}-\mathcal{I}_{t,M_{N+1}}u_{N+1})\|_{I_{N+1}}+E_{T_0}^{\frac{1}{2}}\\
\leq& ch_{N+1}^{r-\frac{1}{2}}M_{N+1}^{-r}\|\partial_t^r u_{N+1}\|_{I_{N+1}}+ch_{N+1}^{r-\frac{1}{2}}M_{N+1}^{\frac{3}{2}-r}\|\partial_t^r u_{N+1}\|_{I_{N+1}}+E_{T_0}^{\frac{1}{2}}\\
\leq& ch^{r-\frac{1}{2}}M^{\frac{3}{2}-r}\|\partial_t^r u_{N+1}\|_{I_{N+1}}+E_{T_0}^{\frac{1}{2}}.
\end{aligned} \tag{A.43}$$

https://doi.org/10.4208/cicp.OA-2016-0181 Published online by Cambridge University Press

Employing the similar argument as above, we can also get

$$|\widetilde{E}'_{N+1}(t_N)| \leq ch^{r-\frac{3}{2}} M^{\frac{7}{2}-r} \|\partial_t^r u_{N+1}\|_{I_{N+1}} + (E'_{T_0})^{\frac{1}{2}}. \tag{A.44}$$

Hence, inserting (A.43) and (A.44) into (A.41) yields

$$\|\widetilde{E}_{N+1}\|_{I_{N+1}} \leq ch^r M^{\frac{7}{2}-r} \|\partial_t^r u_{N+1}\|_{I_{N+1}} + h^{\frac{1}{2}} E_{T_0}^{\frac{1}{2}} + h^{\frac{3}{2}} (E'_{T_0})^{\frac{1}{2}}. \tag{A.45}$$

And the combination of (A.37), (A.44) and (A.45) gives

$$\|\widetilde{E}'_{N+1}\|_{I_{N+1}} \leq ch^{r-1} M^{\frac{7}{2}-r} \|\partial_t^r u_{N+1}\|_{I_{N+1}} + h^{\frac{3}{2}} E_{T_0}^{\frac{1}{2}} + h^{\frac{1}{2}} (E'_{T_0})^{\frac{1}{2}}. \tag{A.46}$$

Furthermore, by Lemma A.1, (A.45) and (A.46) we have

$$\begin{aligned} \|u_{N+1} - U_{N+1}\|_{I_{N+1}}^2 &\leq 2\|\mathcal{I}_{t,M_{N+1}} u - u_{N+1}\|_{I_{N+1}}^2 + 2\|\widetilde{E}_{N+1}\|_{I_{N+1}}^2 \\ &\leq ch^{2r} M^{7-2r} \|\partial_t^r u_{N+1}\|_{I_{N+1}}^2 + chE_{T_0} + ch^3 E'_{T_0}, \end{aligned} \tag{A.47}$$

and

$$\begin{aligned} \|u'_{N+1} - U'_{N+1}\|_{I_{N+1}}^2 &\leq 2\|(\mathcal{I}_{t,M_{N+1}} u)' - u'_{N+1}\|_{I_{N+1}}^2 + 2\|\widetilde{E}'_{N+1}\|_{I_{N+1}}^2 \\ &\leq ch^{2r-2} M^{7-2r} \|\partial_t^r u_{N+1}\|_{I_{N+1}}^2 + chE'_{T_0} + ch^3 E_{T_0}. \end{aligned} \tag{A.48}$$

Thanks to (A.42), (A.47) and (A.48), we can obtain

$$|u_{N+1}(t_{N+1}) - U_{N+1}(t_{N+1})|^2 \leq ch^{2r-1} M^{7-2r} \|\partial_t^r u_{N+1}\|_{I_{N+1}}^2 + cE_{T_0} + ch^2 E'_{T_0}.$$

Similarly, owing to (A.42), (A.46) and (A.36), we have

$$\begin{aligned} &|u'_{N+1}(t_{N+1}) - U'_{N+1}(t_{N+1})|^2 \\ \leq& 2h^{-1}(\|(u_{N+1} - \mathcal{I}_{t,M_{N+1}} u)'\|_{I_{N+1}}^2 + \|\widetilde{E}'_{N+1}\|_{I_{N+1}}^2) \\ &+ 2h(\|(u_{N+1} - \mathcal{I}_{t,M_{N+1}} u)''\|_{I_{N+1}}^2 + \|\widetilde{E}''_{N+1}\|_{I_{N+1}}^2) \\ \leq& ch^{2r-3} M^{7-2r} \|\partial_t^r u_{N+1}\|_{I_{N+1}}^2 + cE'_{T_0} + ch^2 E_{T_0}. \end{aligned}$$

Implementing the above argument recursively on I_n, we arrive at

$$\|u_n - U_n\|_{I_n}^2 \leq ch^{2r} M^{7-2r} \|\partial_t^r u\|_{L^2[T_0,t_n]}^2 + chE_{T_0} + ch^3 E'_{T_0}, \tag{A.49}$$

$$\|(u_n - U_n)'\|_{I_n}^2 \leq ch^{2r-2} M^{7-2r} \|\partial_t^r u\|_{L^2[T_0,t_n]}^2 + chE'_{T_0} + ch^3 E_{T_0}, \tag{A.50}$$

$$|u(t_n) - U_n(t_n)|^2 \leq ch^{2r-1} M^{7-2r} \|\partial_t^r u\|_{L^2[T_0,t_n]}^2 + cE_{T_0} + ch^2 E'_{T_0}, \tag{A.51}$$

$$|u'(t_n) - U'(t_n)|^2 \leq ch^{2r-3} M^{7-2r} \|\partial_t^r u\|_{L^2[T_0,t_n]}^2 + cE'_{T_0} + ch^2 E_{T_0}. \tag{A.52}$$

The required estimates then follow from Theorem 4.1 and (A.49)-(A.52) readily.

https://doi.org/10.4208/cicp.OA-2016-0181 Published online by Cambridge University Press

References

[1] A. H. Bhrawy and A. S. Alofi, A Jacobi-Gauss collocation method for solving nonlinear Lane-Emden type equations, Commun. Nonlinear. Sci. Numer. Simulat., 17 (2012), 62-70.

[2] H. Brunner, Collocation Methods for Volterra Integral and Related Functional Equations, Cambridge University Press, Cambridge, 2004.

[3] C. Canuto, M. Y. Hussaini, A. Quarteroni and T. A. Zang, Spectral Methods: Fundamentals in Single Domains, Springer, Berlin, 2006.

[4] S. Chandrasekhar, Introduction to the Study of Stellar Structure, Dover, New York, 1967.

[5] E. H. Doha, A. H. Bhrawy, R. M. Hafez and R. A. Van Gorder, A Jacobi rational pseudospectral method for Lane-Emden initial value problems arising in astrophysics on a semi-infinite interval, Comp. Appl. Math., 33 (2014), 607-619.

[6] E. H. Doha, A. H. Bhrawy, R. M. Hafez and R. A. Van Gorder, Jacobi rational-Gauss collocation method for Lane-Emden equations of astrophysical significance, Nonlinear. Anal-Model., 19 (2014), 1-14.

[7] B. Gürbü and M. Sezer, Laguerre polynomial approach for solving Lane-Emden type functional differential equations, Appl. Math. Comput., 242 (2014), 255-264.

[8] B. Y. Guo, Spectral and pseudospectral methods for unbounded domains (in Chinese), Sci. Sin. Math., 45 (2015), 975-1024.

[9] B. Y. Guo and Z. Q. Wang, Legendre-Gauss collocation methods for ordinary differential equations, Adv. Comput. Math., 30 (2009), 249-280.

[10] B. Y. Guo and J. P. Yan, Legendre-Guass collocation for initial value problems of second order ordinary differential equations, Appl. Numer. Math., 59 (2009), 1386-1408.

[11] G.P. Horedt, Polytropes: Applications in Astrophysics and Related Fields, Kluwer Academic Publishers, Dordrecht, 2004.

[12] S. G. Hosseini and S. Abbasbandy, Solution of Lane Emden Type Equations by Combination of the Spectral Method and Adomian Decomposition Method, Math. Prob. Eng., Volume 2015, Article ID 534754, 10 pages.

[13] A. Nazari-Golshan, S.S. Nourazar, H. Ghafoori-Fard, A. Yildirim and A. Campo, A modified homotopy perturbation method coupled with the Fourier transform for nonlinear and singular Lane-Emden equations, Appl. Math. Lett., 26 (2013), 1018-1025.

[14] K. Parand, M. Dehghan, A. Rezaeia and S. Ghaderi, An approximation algorithm for the solution of the nonlinear Lane-Emden type equations arising in astrophysics using Hermite functions collocation method, Comput. Phys. Commun., 181 (2010), 1096-1108.

[15] K. Parand, M. Shahini and M. Dehghan, Rational Legendre pseudospectral approach for solving nonlinear differential equations of Lane-Emden type, J. Comput. Phys., 228 (2009), 8830-8840.

[16] R. Rach, A. M. Wazwaz and J. S. Duan, The Volterra integral form of the Lane-Emden equation: new derivations and solution by the Adomian decomposition method, J. Appl. Math. Comput., 47 (2015), 365-379.

[17] O. U. Richardson, The Emission of Electricity from Hot Bodies, Longman's Green and Company, London, 1921.

[18] P. K. Sahu and S. Saha Ray, Numerical solutions for integro-differential forms of Lane-Emden equations of first and second kind using Legendre Multi-Wavelets, Electron. J. Differ. Eq., 28 (2015), 1-11.

[19] J. Shen, T. Tang and L. L. Wang, Spectral Methods: Algorithms, Analysis and Applications, Springer, Berlin, 2011.

https://doi.org/10.4208/cicp.OA-2016-0181 Published online by Cambridge University Press

[20] C. T. Sheng, Z. Q. Wang and B. Y. Guo, A multistep Legendre-Gauss spectral collocation method for nonlinear Volterra integral equations, SIAM J. Numer. Anal., 52 (2014), 1953-1980.
[21] Z. Q. Wang, Y. L. Guo and L. J. Yi, An *hp*-version Legendre-Jacobi spectral collocation method for Volterra integro-differential equations with smooth and weakly singular kernels, Math. Comp., in press.
[22] A. M. Wazwaz, Linear and Nonlinear Intergral Equations Methods and Applications, Higher Education Press, Beijing, 2011.
[23] A. M. Wazwaz, The variational iteration method for solving the Volterra integro-differential forms of the Lane-Emden equations of the first and the second kind, J. Math. Chem., 52 (2014), 613-626.
[24] J. P. Yan and B. Y. Guo, Laguerre-Gauss collocation method for initial value problems of second order ODEs, Appl. Math. Mech. Engl. Ed., 32 (2011), 1541-1564.
[25] L. J. Yi and Z. Q. Wang, A Legendre-Gauss-Radau spectral collocation method for first order nonlinear delay differential equations, Calcolo, 53(2016), 691-721.
[26] Y. H. Youssri, W. M. Abd-Elhameed and E. H. Doha, Ultraspherical Wavelets method for solving Lane-Emden type equations, Rom. Journ. Phys., 60 (2015), 1298-1314.

https://doi.org/10.4208/cicp.OA-2016-0181 Published online by Cambridge University Press